

A colitogenic memory CD4⁺ T cell population mediates gastrointestinal graft-versus-host disease

Vivian Zhou,¹ Kimberle Agle,¹ Xiao Chen,¹ Amy Beres,² Richard Komorowski,³ Ludovic Belle,¹ Carolyn Taylor,¹ Fenlu Zhu,¹ Dipica Haribhai,⁴ Calvin B. Williams,⁴ James Verbsky,⁴ Wendy Blumenschein,⁵ Svetlana Sadekova,⁵ Eddie Bowman,⁵ Christie Ballantyne,⁶ Casey Weaver,⁷ David A. Serody,⁸ Benjamin Vincent,⁸ Jonathan Serody,⁸ Daniel J. Cua,⁵ and William R. Drobyski^{1,2,4}

¹Department of Medicine, ²Department of Microbiology, ³Department of Pathology, and ⁴Department of Pediatrics, Medical College of Wisconsin, Milwaukee, Wisconsin, USA. ⁵Merck Pharmaceuticals, Palo Alto, California, USA. ⁶Baylor College of Medicine, Houston, Texas, USA. ⁷University of Alabama–Birmingham, Birmingham, Alabama, USA. ⁸University of North Carolina, Chapel Hill, North Carolina, USA.

Damage to the gastrointestinal tract is a major cause of morbidity and mortality in graft-versus-host disease (GVHD) and is attributable to T cell–mediated inflammation. In this work, we identified a unique CD4⁺ T cell population that constitutively expresses the β_2 integrin CD11c and displays a biased central memory phenotype and memory T cell transcriptional profile, innate-like properties, and increased expression of the gut-homing molecules $\alpha_4\beta_7$ and CCR9. Using several complementary murine GVHD models, we determined that adoptive transfer and early accumulation of β_2 integrin–expressing CD4⁺ T cells in the gastrointestinal tract initiated Th1-mediated proinflammatory cytokine production, augmented pathological damage in the colon, and increased mortality. The pathogenic effect of this CD4⁺ T cell population critically depended on coexpression of the IL-23 receptor, which was required for maximal inflammatory effects. Non-Foxp3-expressing CD4⁺ T cells produced IL-10, which regulated colonic inflammation and attenuated lethality in the absence of functional CD4⁺Foxp3⁺ T cells. Thus, the coordinate expression of CD11c and the IL-23 receptor defines an IL-10–regulated, colitogenic memory CD4⁺ T cell subset that is poised to initiate inflammation when there is loss of tolerance and breakdown of mucosal barriers.

Introduction

Graft-versus-host disease (GVHD) is a proinflammatory syndrome that is initiated by donor T cells and is the major complication of allogeneic hematopoietic stem cell transplantation (1–3). The overproduction of inflammatory cytokines is a critical component of this process and is able to mediate pathological damage directly, or indirectly by activation and/or recruitment of other effector cell populations (4–6). During the acute phase, GVHD generally targets a restricted set of organs, which include the skin, liver, and gastrointestinal (GI) tract. Of these tissues sites, the GI tract is of particular relevance in the pathophysiology of this disorder, as damage to this organ plays a crucial role in the amplification of systemic GVHD severity (3, 7). This is attributable to breakdown of the mucosal barrier, which leads to increased systemic proinflammatory cytokine secretion arising from interactions between bacterial products (e.g., endotoxin) and donor-derived immune effector cells that are resident in the GI tract (8). Clinically, this damaged mucosal barrier predisposes patients to infectious complications that can be life-threatening.

Within the GI tract in both GVHD and other inflammatory bowel diseases, interleukin 23 (IL-23) has emerged as a pivotal cytokine

that sits at the apex of a proinflammatory cytokine cascade and is directly responsible for the ensuing tissue damage that occurs in these disorders (9, 10). Secretion of IL-23 by activated antigen-presenting cells results in widespread inflammatory cytokine production as well as activation and expansion of immune effector cell populations. Signaling of IL-23 occurs by binding of the cytokine to an IL-23 receptor (IL-23R) complex that is composed of IL-12R β 1 and a unique IL-23R subunit and is expressed on CD4⁺ T cells, monocytes/macrophages, dendritic cells, and other members of the innate immune system (11). Thus, IL-23 is able to mediate proinflammatory effects in the GI tract through both the innate and adaptive arms of the immune system (10, 12), although the relative importance of each component is not completely understood. The severity of GVHD is also a function of the balance between effector and regulatory arms of the immune system (13, 14). The absence of regulatory cell populations has been shown to exacerbate GVHD severity (15, 16), indicating that counterregulatory mechanisms are operative during GVHD, although often insufficient to prevent or mitigate the disease. The precise pathways by which the proinflammatory effects of IL-23 are regulated within the colon microenvironment, however, have not been well delineated.

Herein, we used multiple murine models of GVHD to delineate the specific immune cell populations that mediate the proinflammatory effects of IL-23 within the colon and to determine how inflammation mediated through IL-23/IL-23R signaling was regulated. During the course of these studies, we identified a novel subset of CD4⁺IL-23R⁺ T cells that constitutively expresses the β_2 integrin CD11c and demonstrated that these cells constitute a highly pathogenic CD4⁺ T cell population that

Authorship note: V. Zhou and K. Agle contributed equally to this work.

Note regarding evaluation of this manuscript: Manuscripts authored by scientists associated with Duke University, The University of North Carolina at Chapel Hill, Duke-NUS, and the Sanford-Burnham Medical Research Institute are handled not by members of the editorial board but rather by the science editors, who consult with selected external editors and reviewers.

Conflict of interest: D.J. Cua is employed by Merck Research Labs.

Submitted: November 4, 2015; **Accepted:** June 9, 2016.

Reference information: *J Clin Invest*. 2016;126(9):3541–3555. doi:10.1172/JCI80874.

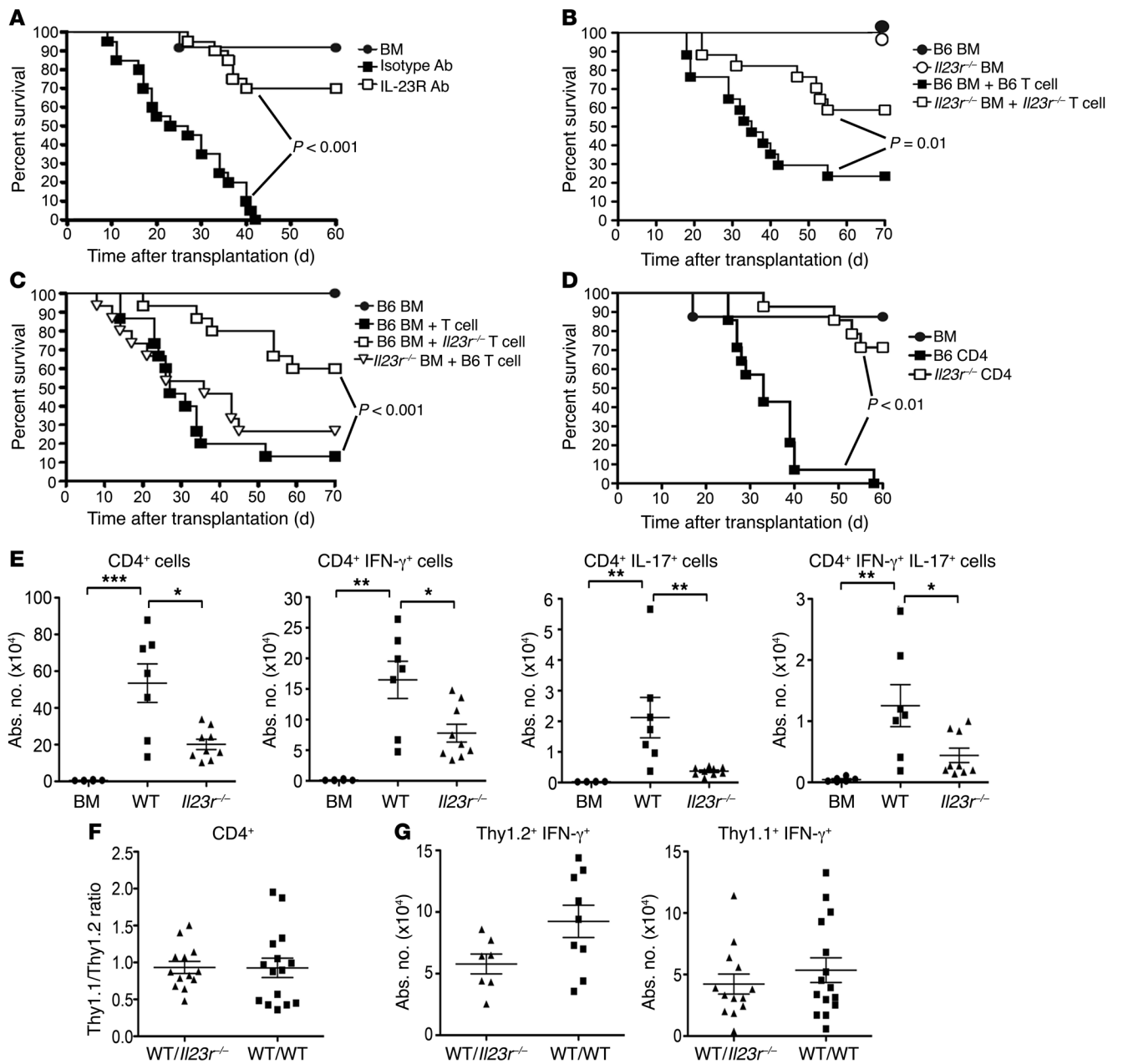


Figure 1. CD4⁺IL-23R⁺ T cells drive inflammation in the colon during GVHD. (A) BALB/c mice were transplanted with B6 BM alone (black circles, $n = 12$) or with B6 spleen cells. Animals transplanted with spleen cells were treated with an isotype control (black squares, $n = 20$) or anti-IL-23R antibody (white squares, $n = 20$). (B) BALB/c mice transplanted with BM from B6 (black circles, $n = 12$) or *Il23r^{-/-}* (white circles, $n = 12$) donors or BM and spleen cells from B6 (black squares, $n = 17$) or *Il23r^{-/-}* animals (white squares, $n = 17$). (C) BALB/c mice transplanted with B6 T cell depletion (TCD) BM cells (black circles, $n = 9$), B6 TCD BM plus 0.6×10^6 to 1.2×10^6 purified B6 T cells (black squares, $n = 15$), B6 TCD BM plus an equivalent number of *Il23r^{-/-}* T cells (white squares, $n = 15$), or *Il23r^{-/-}* TCD BM and B6 T cells (white triangles, $n = 15$). (D) BALB/c mice transplanted with B6 Rag-1 BM (black circles, $n = 8$) or with CD4⁺ T cells from B6 *Il23r^{-/-}* (black squares, $n = 14$) or *Il23r^{-/-}* animals (white squares, $n = 14$). Survival data are from 3–4 experiments per panel. (E) BALB/c mice transplanted with B6 Rag-1 BM alone (circles, $n = 5$) or with purified CD4⁺ T cells from B6 (squares, $n = 7$) or *Il23r^{-/-}* animals (triangles, $n = 9$). The absolute number of CD4⁺ T cells that secreted IFN- γ and/or IL-17 in the colon 3 weeks after transplantation. (F and G) BALB/c mice transplanted with B6 Rag-1 BM and a 1:1 mixture of CD4⁺ T cells from B6.PL *Il23r^{-/-}* and B6 *Il23r^{-/-}* animals (WT/*Il23r^{-/-}*) (triangles, $n = 7$ –13), or B6 Rag-1 BM and a mixture of CD4⁺ T cells from B6.PL *Il23r^{-/-}* and B6 *Il23r^{-/-}* mice (WT/WT) (squares, $n = 9$ –15). Ratio of CD4⁺ Thy1.1⁺/Thy1.2⁺ T cells and absolute number of CD4⁺Thy1.2⁺IFN- γ ⁺ and Thy1.1⁺IFN- γ ⁺ T cells is shown. Data in E–G are from 3 experiments. Statistically significant differences were calculated using the log rank test and 2-tailed Mann-Whitney U test. * $P < 0.05$, ** $P < 0.01$, *** $P < 0.001$.

plays a critical role in colonic inflammation. Moreover, we show that this cell population has a biased central memory T cell phenotype, a memory T cell transcriptional profile, and increased expression of gut-homing molecules, which poises them for

early entry into the GI tract under inflammatory conditions. Additionally, we demonstrate that these cells are primarily regulated by IL-10 that is produced by CD4⁺ non-Foxp3-expressing conventional T cells. Finally, our studies reveal that CD11c

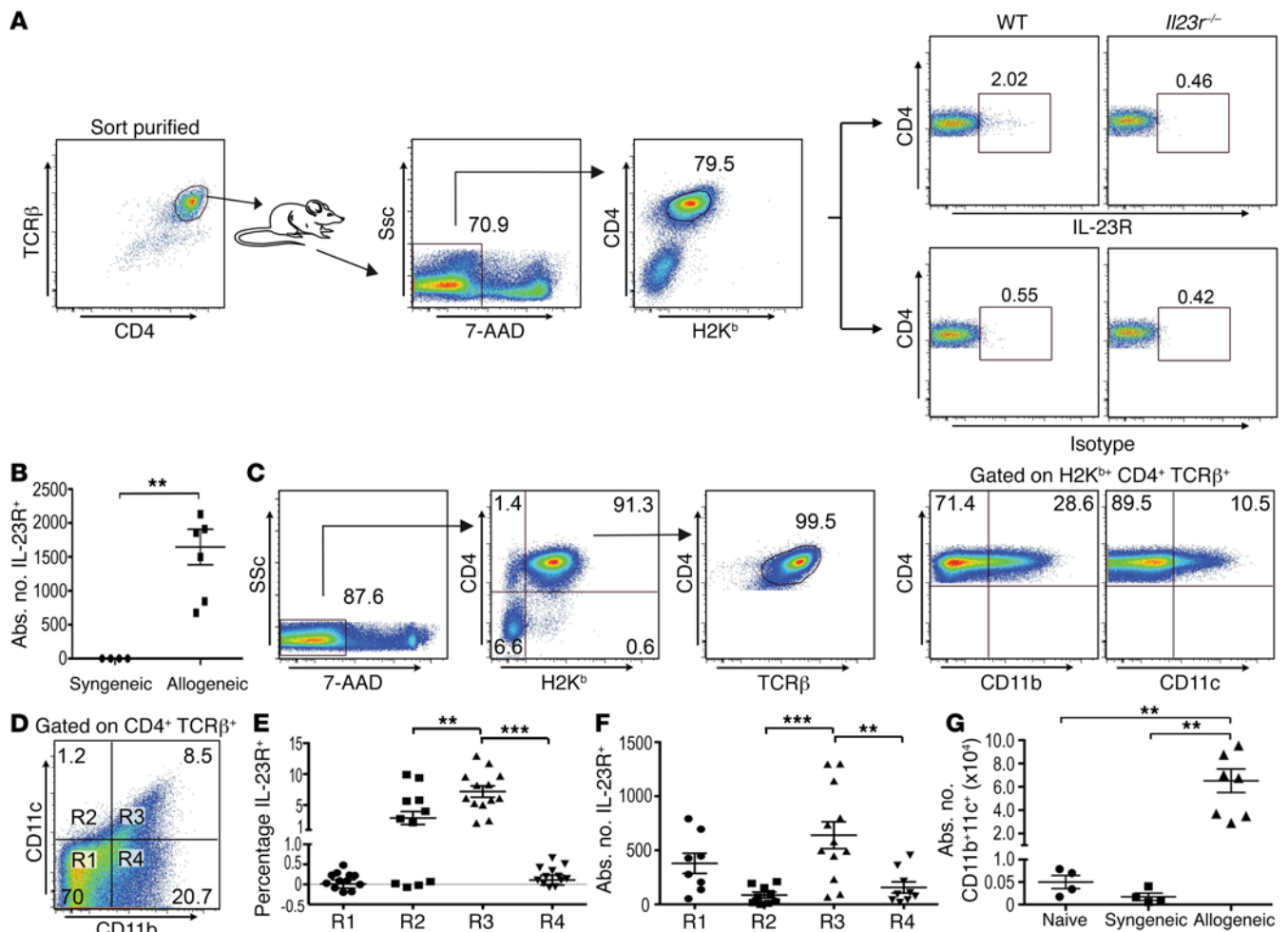


Figure 2. CD11b and CD11c expression marks a CD4⁺IL-23R⁺ T cell population that accumulates early in the colon early during GVHD. (A) Irradiated BALB/c mice were reconstituted with 3×10^6 to 4×10^6 sort-purified B6 CD4⁺αβ⁺ T cells. Representative dot plot of IL-23R expression gated on 7-aminoactinomycin-negative (7-AAD⁻) donor-derived CD4⁺ T cells from the colon 5 days after transplantation. Staining with an isotype control is shown for comparison. IL-23R expression on colonic CD4⁺ T cells from BALB/c mice transplanted with CD4⁺ *Il23r*^{-/-} T cells is shown to confirm antibody specificity. (B) Absolute number of CD4⁺IL-23R⁺ T cells in the colon of syngeneic (B6.PL→B6) ($n = 4$) versus allogeneic (B6→BALB/c) ($n = 7$) recipients. Data are from 2 experiments. (C) Representative dot plot of CD11b and CD11c expression on gated 7-AAD⁻ donor-derived CD4⁺αβ⁺ T cells isolated from the colon of allogeneic recipients 5 days after transplantation. (D) Representative dot plot of CD11b and CD11c coexpression on donor-derived CD4⁺αβ⁺ T cells from C. (E and F) Percentage and absolute number of CD4⁺IL-23R⁺ T cells from the 4 quadrants (i.e., R1–R4) depicted in D. Calculations were performed by subtraction of the percentage of cells that stained positively for the isotype control from the percentage that were IL-23R⁺. Data are from 4 experiments ($n = 12$ –13 animals). (G) Irradiated B6.PL ($n = 4$) or BALB/c ($n = 12$) mice reconstituted with 4×10^6 purified B6 CD4⁺ T cells. The absolute number of donor CD4⁺ T cells that expressed CD11b and/or CD11c in the colon is shown. Normal nontransplanted (naive) B6 mice ($n = 4$) served as controls. Data are from 2 experiments. Statistically significant differences were calculated using the 2-tailed Mann-Whitney *U* test. ** $P < 0.01$, *** $P < 0.001$.

is constitutively expressed on human CD4⁺ T cells and undergoes increased expression after activation, indicating that this phenotype may therefore contribute to the pathophysiology of colonic inflammation in humans.

Results

IL-23 mediates GVHD lethality and pathological damage in the colon through direct effects on CD4⁺IL-23R⁺ donor T cells. To determine the functional significance of IL-23R expression on donor cells, we used antibody-based and genetic approaches to examine the effect of this signaling pathway on GVHD severity. Lethally irradiated recipients treated with anti-IL-23R antibody had significantly prolonged survival compared with mice to which control antibody was administered (Figure 1A). Similarly, whereas the majori-

ty of animals reconstituted with marrow grafts from wild-type donors died from GVHD, mice transplanted with *Il23r*^{-/-} grafts had increased survival (Figure 1B). Histological analysis indicated that there was reduced inflammation within the colon, but no difference in pathological scores in the liver or lung (Supplemental Figure 1, A and B; supplemental material available online with this article; doi:10.1172/JCI80874DS1), consistent with prior observations of preferential protection within this tissue site after blockade of IL-23 signaling (9). Prior studies had shown that IL-23R gene expression levels were augmented in CD11c⁺CD11b⁺ cells, CD11c⁺CD11b⁺ cells, and CD4⁺ T cells obtained from the colons of mice with GVHD (9), indicating that cells of the innate and adaptive arms of the immune system were responsive to IL-23 signaling. Experiments performed to delineate the critical IL-23R-

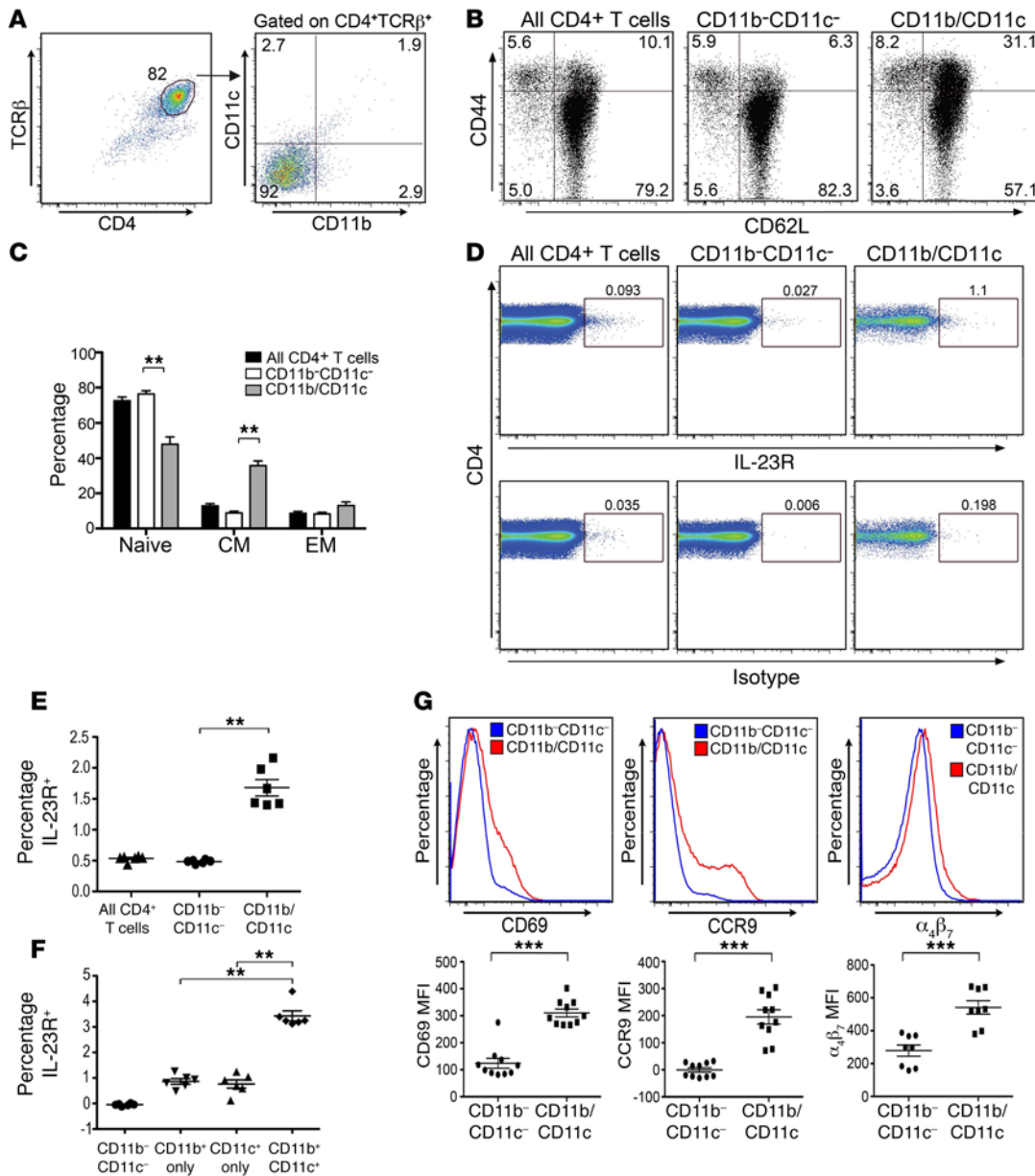


Figure 3. β_2 Integrin-expressing CD4⁺ T cells have a biased central memory phenotype and increased expression of gut-homing molecules. (A) Representative dot plot depicting CD11b and CD11c expression on gated CD4⁺TCR β ⁺ T cells pooled from spleen and lymph nodes (peripheral and mesenteric) of a normal B6 mouse. (B) Representative dot plots depicting CD44 and CD62L expression on whole CD4⁺ T cells, CD4⁺ T cells that lacked expression of either β_2 integrin, or CD4⁺ T cells that expressed at least 1 of the 2 β_2 integrins. (C) Percentage of naive, central memory (CM), and effector memory (EM) CD4⁺ T cells in populations shown in B (*n* = 5 mice per group). Data are presented as the mean \pm SEM. (D) Representative dot plots depicting IL-23R expression and background isotype staining on CD4⁺TCR β ⁺ T cells, CD4⁺ T cells that did not express either CD11b or CD11c, or CD4⁺ T cells that expressed at least 1 of these 2 β_2 integrins. (E) Scatterplot of percentage of each cell population noted in D that expressed the IL-23R (*n* = 6 mice per group). (F) Scatterplot of the percentage of naive CD4⁺ T cells lacking expression of either β_2 integrin or expressing CD11b alone, CD11c alone, or both CD11b and CD11c (*n* = 6/group) that expressed the IL-23R. (G) Representative histograms and scatterplots of mean fluorescence intensity of CD69, CCR9, and $\alpha_4\beta_7$ expression on CD4⁺ T cells that lacked expression of either β_2 integrin or CD4⁺ T cells that expressed at least 1 of these 2 integrins. Statistically significant differences were calculated using the log rank test and 2-tailed Mann-Whitney *U* test. ***P* < 0.01, ****P* < 0.001.

expressing population revealed that survival was significantly prolonged in animals that were transplanted with *Il23r*^{-/-} T cells, whereas mortality was unaffected when IL-23R expression was absent from BM-derived cells (Figure 1C), indicating that T cell expression of the IL-23R was critical. Since the IL-23R has been reported to be expressed on CD4⁺, but not CD8⁺, T cells (11), we compared the ability of CD4⁺ *Il23r*^{+/+} and *Il23r*^{-/-} T cells to medi-

ate lethal GVHD. Transplantation with CD4⁺ T cells from *Il23r*^{-/-} animals resulted in less GVHD-associated mortality (Figure 1D) and a significant reduction in mRNA levels of the inflammatory cytokines IFN- γ , IL-6, and IL-17, but not IL-22 (Supplemental Figure 1C). The absolute numbers of CD4⁺, CD4⁺IFN- γ ⁺, CD4⁺IL-17⁺, and CD4⁺IFN- γ ⁺IL-17⁺ T cells were also significantly reduced in the colons of these mice (Figure 1E). We then examined whether

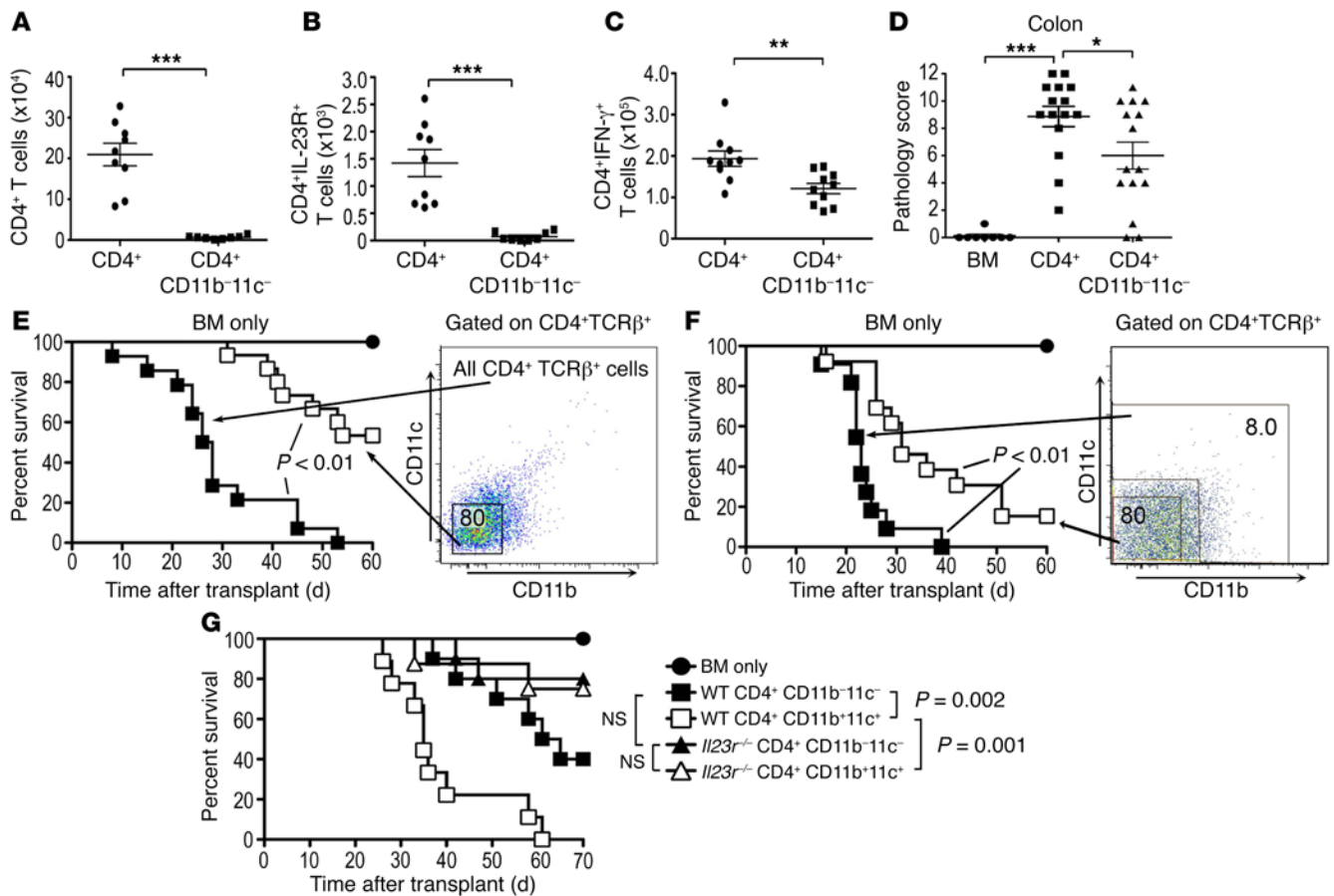


Figure 4. Pathogenicity of β_2 integrin-expressing CD4⁺ T cells is dependent on the coexpression of the IL-23R. (A and B) BALB/c mice transplanted with 4×10^6 CD4⁺ $\alpha\beta^+$ T cells (circles) ($n = 9$) or CD4⁺ $\alpha\beta^+$ CD11b⁻CD11c⁻ (squares) ($n = 8$) T cells. Total number of CD4⁺ (A) and CD4⁺IL-23R⁺ T cells (B) in the colon on day 5 is shown. Data are cumulative results from 2 experiments. (C) Total number of CD4⁺IFN- γ^+ T cells in the colon on day 10 in mice transplanted with 1.5×10^6 CD4⁺ $\alpha\beta^+$ T cells (circles, $n = 10$) or CD4⁺ $\alpha\beta^+$ CD11b⁻CD11c⁻ T cells (squares, $n = 10$). Data are from 2 experiments. (D) Pathology scores in the colon of mice transplanted with B6 Rag-1 BM alone (circles, $n = 8$) or together with CD4⁺ $\alpha\beta^+$ (squares, $n = 15$) or CD4⁺CD11b⁻CD11c⁻ (triangles, $n = 15$) T cells 21 days after transplantation. Data are from 3 experiments. (E) BALB/c mice transplanted with B6 Rag-1 BM alone (black circles, $n = 9$) or with 1×10^6 sorted CD4⁺ $\alpha\beta^+$ (black squares, $n = 14$) or CD4⁺ $\alpha\beta^+$ CD11b⁻CD11c⁻ (white squares, $n = 14$) T cells. Data are from 3 experiments. (F) BALB/c mice transplanted with B6 Rag-1 BM alone (black circles, $n = 9$) or with CD4⁺ $\alpha\beta^+$ T cells that expressed CD11b⁺ and/or CD11c⁺ (black squares, $n = 11$) or CD4⁺ $\alpha\beta^+$ CD11b⁻CD11c⁻ T cells (white squares, $n = 13$). Data are from 3 experiments. (G) BALB/c mice transplanted with B6 Rag-1 BM alone (black circles, $n = 7$) or with either 1×10^6 CD4⁺CD11b⁻CD11c⁻ T cells (black squares, $n = 10$), CD4⁺ T cells that expressed CD11b and/or CD11c (white squares, $n = 9$), CD4⁺ *Il23r*^{-/-} CD11b⁻CD11c⁻ T cells (black triangles, $n = 10$), or CD4⁺ *Il23r*^{-/-} T cells that expressed CD11b and/or CD11c (white triangles, $n = 8$). Data are from 2 experiments. Statistically significant differences were calculated using the log rank test and 2-tailed Mann-Whitney *U* test. * $P < 0.05$, ** $P < 0.01$, *** $P < 0.001$.

CD4⁺ *Il23r*^{-/-} T cells were intrinsically defective in their ability to accumulate in the colons of animals with GVHD using congenically marked *Il23r*^{+/+} and *Il23r*^{-/-} T cells. Using Thy1 allelic differences to distinguish Thy1.1⁺ *Il23r*^{+/+} from Thy1.2⁺ *Il23r*^{-/-} CD4⁺ T cells, we observed that there was no difference in the ratio of Thy1.2⁺ to Thy1.1⁺ CD4⁺ T cells (Figure 1F) or the absolute number of Thy1.2⁺ versus Thy1.1⁺ CD4⁺ T cells that were capable of secreting IFN- γ (Figure 1G) in the colons of transplanted animals. Collectively, these studies indicated that the T cell-directed inflammatory effects of IL-23 within the colon were mediated primarily by CD4⁺ IL-23R-expressing T cells that were able to drive the accumulation and differentiation of *Il23r*^{-/-} T cells into a proinflammatory phenotype through a cell-extrinsic mechanism.

CD4⁺IL-23R⁺ T cells in the colon coexpress the β_2 integrins CD11b and CD11c. The ability of CD4⁺IL-23R⁺ T cells to induce inflammation in the colon led us to further characterize these cells. We observed that a small population of CD4⁺IL-23R⁺ T cells (~1%)

could be identified in the colon of GVHD animals as early as 5 days after transplantation (Figure 2A). The specificity of the anti-IL-23R antibody was confirmed by demonstration that colonic CD4⁺ T cells obtained from recipients that were reconstituted with CD4⁺ T cells from *Il23r*^{-/-} mice had no detectable expression of the receptor (Figure 2A). These cells were also present in significantly higher numbers in comparison with recipients of syngeneic marrow grafts (Figure 2B). Additional phenotypic characterization of CD4⁺ T cells in this tissue site revealed a population of donor-derived CD4⁺ $\alpha\beta^+$ T cells that expressed the β_2 integrins CD11b and CD11c (Figure 2C). The majority of these cells expressed CD11b alone; however, there were defined populations that also expressed CD11c alone or both CD11b and CD11c (Figure 2D). To determine whether there was any correlation between IL-23R and β_2 integrin expression, we examined CD4⁺ T cells from each of these 4 quadrants (i.e., R1-R4) for concurrent IL-23R expression. These studies revealed that the frequency and absolute number of IL-23R-expressing CD4⁺ T cells

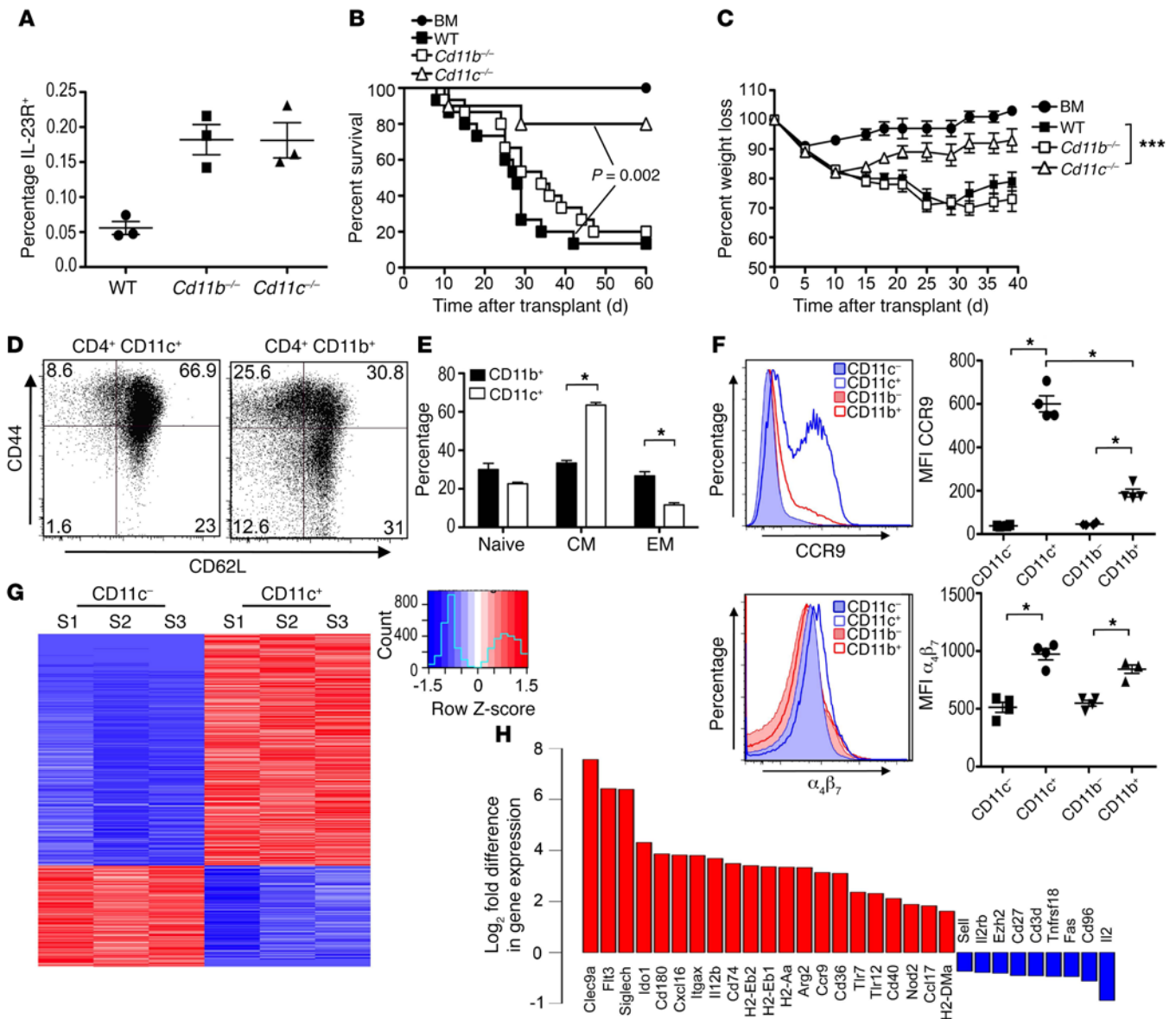


Figure 5. CD4⁺CD11c⁺ T cells drive inflammation in the colon during GVHD. (A) Baseline IL-23R expression on gated CD4⁺ T cells from the spleen and lymph nodes of normal wild-type, *Cd11b*^{-/-}, or *Cd11c*^{-/-} mice. (B and C) BALB/c mice transplanted with B6 Rag-1 BM alone (black circles, *n* = 9) or with 0.8 × 10⁶ CD4⁺ T cells from wild-type (black squares, *n* = 15), *Cd11b*^{-/-} (white squares, *n* = 15), or *Cd11c*^{-/-} (white triangles, *n* = 10) animals. Overall survival and serial weight curves are shown. (D) Representative dot plot depicting CD44 and CD62L expression on gated CD4⁺CD11c⁺ and CD4⁺CD11b⁺ T cells from *Cd11b*^{-/-} and *Cd11c*^{-/-} animals, respectively. (E) Percentage of CD4⁺CD11b⁺ (black bars) and CD4⁺CD11c⁺ (white bars) T cells with naive, central memory (CM), or effector memory (EM) phenotypes (*n* = 4). Data are presented as mean ± SEM. (F) Representative histograms of CCR9 and $\alpha_4\beta_7$ expression on CD4⁺ T cells from *Cd11b*^{-/-} (blue) or *Cd11c*^{-/-} (pink) mice based on presence (open histograms) or absence (filled histograms) of CD11b or CD11c. Scatterplots of mean fluorescence intensity of CCR9 and $\alpha_4\beta_7$ expression on CD4⁺ T cells from replicate animals are also depicted. (G) Hierarchical clustering of 684 genes that were significantly regulated in flow-sorted CD4⁺CD11c⁺CD44^{hi}CD62L⁺ versus CD4⁺CD11c⁺CD44^{hi}CD62L⁻ T cells from wild-type mice. S1–S3 refer to independent replicate samples with each replicate derived from pooled spleen and lymph node cells from 3–4 mice. Z score denotes SD. (H) Waterfall plot showing log₂ fold difference in gene expression of differentially regulated genes. Red bars denote genes that had increased expression in CD4⁺CD11c⁺CD44^{hi}CD62L⁺ T cells, while blue bars depict genes with decreased expression relative to CD4⁺CD11c⁺CD44^{hi}CD62L⁻ T cells. Statistically significant differences were calculated using the log rank test and 2-tailed Mann-Whitney *U* test. **P* < 0.05, ****P* < 0.001.

were highest in cells that coexpressed CD11b and CD11c (R3 quadrant) (Figure 2, E and F, and Supplemental Figure 2). The absolute number of CD4⁺ T cells that expressed CD11b⁺ and/or CD11c⁺ T cells was also greater in the colon of recipients that received allogeneic marrow grafts when compared with normal mice or recipients of syngeneic grafts (Figure 2G), indicating that these cells arose in the setting of alloreactivity.

Pathogenicity of β_2 integrin-expressing CD4⁺ T cells is dependent on coexpression of the IL-23R. We observed that a small population (~8%) of CD4⁺ T cells obtained from the spleen and lymph nodes of normal mice constitutively expressed CD11b and/or CD11c (Figure 3A). This population was biased toward a CD44^{hi}CD62L^{hi} central memory phenotype when compared with naive CD4⁺ T cells or CD4⁺ T cells that lacked expression of either β_2 integrin (Figure

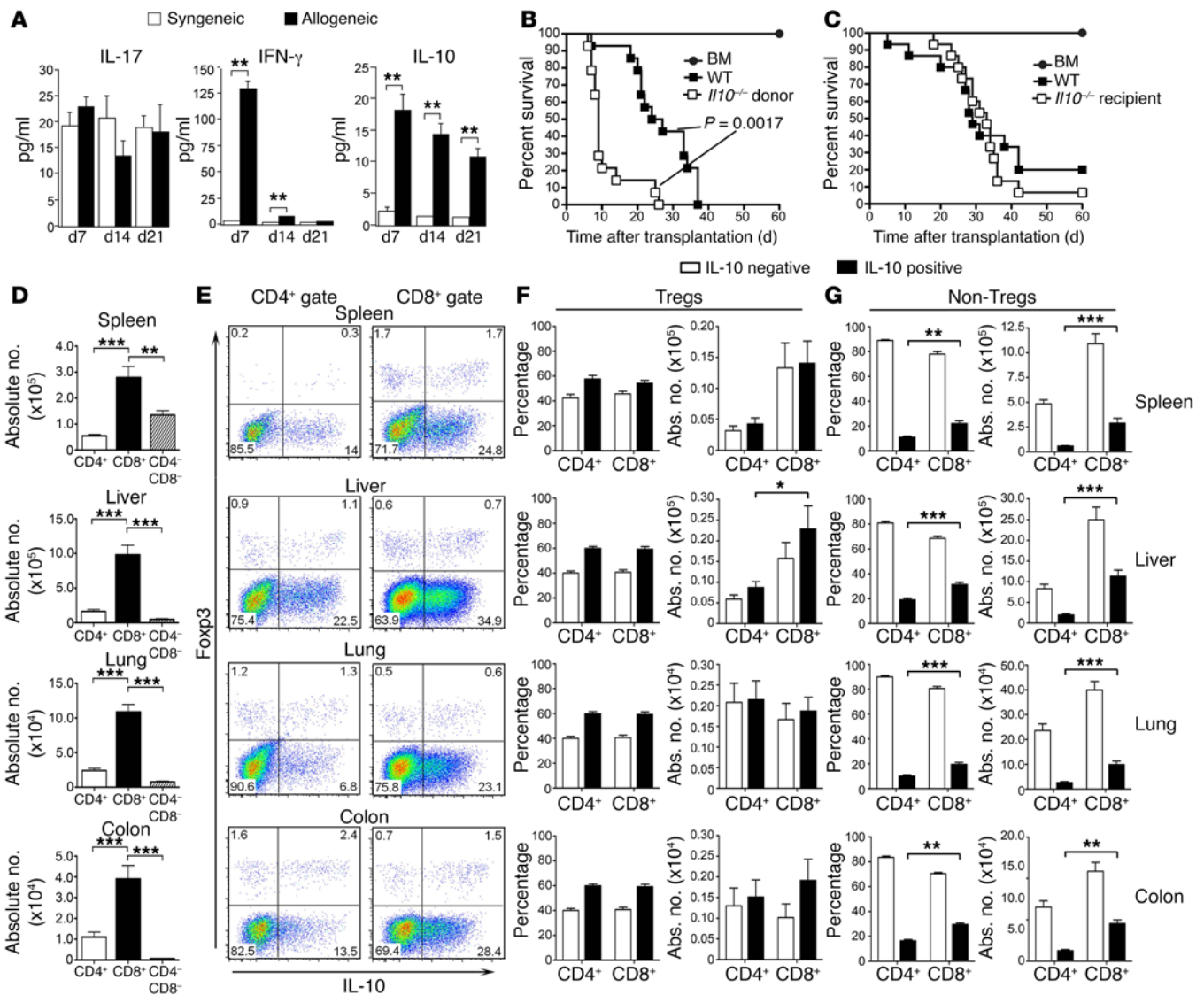


Figure 6. Donor-derived IL-10 regulates GVHD and is produced primarily by non-Foxp3-expressing T cells. (A) BALB/c mice transplanted with BALB/c BM and spleen cells (syngeneic) or an equivalent number of B6 BM and spleen cells (allogeneic). Serum cytokine analysis of IFN- γ , IL-10, and IL-17 levels ($n = 5-9$ per group). Data are derived from 2 experiments and presented as mean \pm SEM. (B) BALB/c mice transplanted with B6 BM alone (black circles, $n = 9$) or with either wild-type B6 (black squares, $n = 14$) or B6 *Il10*^{-/-} (white squares, $n = 14$) spleen cells. Data are cumulative results from 3 experiments. (C) Wild-type BALB/c (black squares, $n = 15$) or *Il10*^{-/-} BALB/c (white squares, $n = 15$) mice transplanted with B6 BM and B6 spleen cells. Wild-type BALB/c mice (black circles, $n = 9$) transplanted with B6 BM cells alone served as controls. Data are cumulative results from 3 experiments. (D) BALB/c mice transplanted with B6 Rag-1 BM and B6 10BiT.Foxp3^{EGFP} spleen cells. The absolute number of donor CD4⁺ (white bars), CD8⁺ (black bars), and CD4⁺CD8⁺ (hatched bars) cells that were IL-10⁺ in the specified tissue sites 10 days after transplantation. Data are from 6-12 mice per group from 3 separate experiments. (E) Representative dot plots depicting the percentage of donor CD4⁺ and CD8⁺ T cells that expressed Foxp3 and IL-10 10 days after transplantation. (F and G) Percentage and absolute number of CD4⁺Foxp3⁺ and CD8⁺Foxp3⁺ T cells (Tregs, F) and CD4⁺Foxp3⁻ and CD8⁺Foxp3⁻ T cells (non-Tregs, G) that were IL-10⁻ (white bars) or IL-10⁺ (black bars) ($n = 8$ per group). Data are presented as mean \pm SEM and are from 2 experiments. Statistically significant differences were calculated using the log rank test and 2-tailed Mann-Whitney *U* test. * $P < 0.05$, ** $P < 0.01$, *** $P < 0.001$.

3, B and C), and also had higher expression of the IL-23R (Figure 3, D and E). Furthermore, IL-23R expression was highest on CD4⁺ T cells that coexpressed both β_2 integrins (Figure 3F). Expression of the activation molecule CD69, and the gut-homing molecules CCR9 and $\alpha_4\beta_7$, was also increased on CD4⁺ T cells that coexpressed CD11b and/or CD11c (Figure 3G). CD11b and CD11c were constitutively expressed on a small percentage of human CD4⁺ T cells, and could be further augmented when cells were stimulated with allogeneic peripheral blood mononuclear cells (Supplemental Figure 3, A and B), indicating that this was not a species-dependent phe-

nomenon. To determine the functional significance of constitutive β_2 integrin expression on CD4⁺ T cells, animals were transplanted with sorted CD4⁺ $\alpha\beta^+$ T cells or CD4⁺ T cells that lacked expression of either CD11b or CD11c. Mice reconstituted with CD4⁺CD11b⁻CD11c⁻ T cells had a significantly reduced number of total donor-derived CD4⁺, CD4⁺IL-23R⁺, and CD4⁺IFN- γ ⁺ T cells in the colon (Figure 4, A-C), indicating that expression of these specific integrins was important for the accumulation of proinflammatory CD4⁺IL-23R⁺ T cells in the colon. Furthermore, we noted that pathological damage in the colon was significantly reduced in this cohort (Figure 4D),

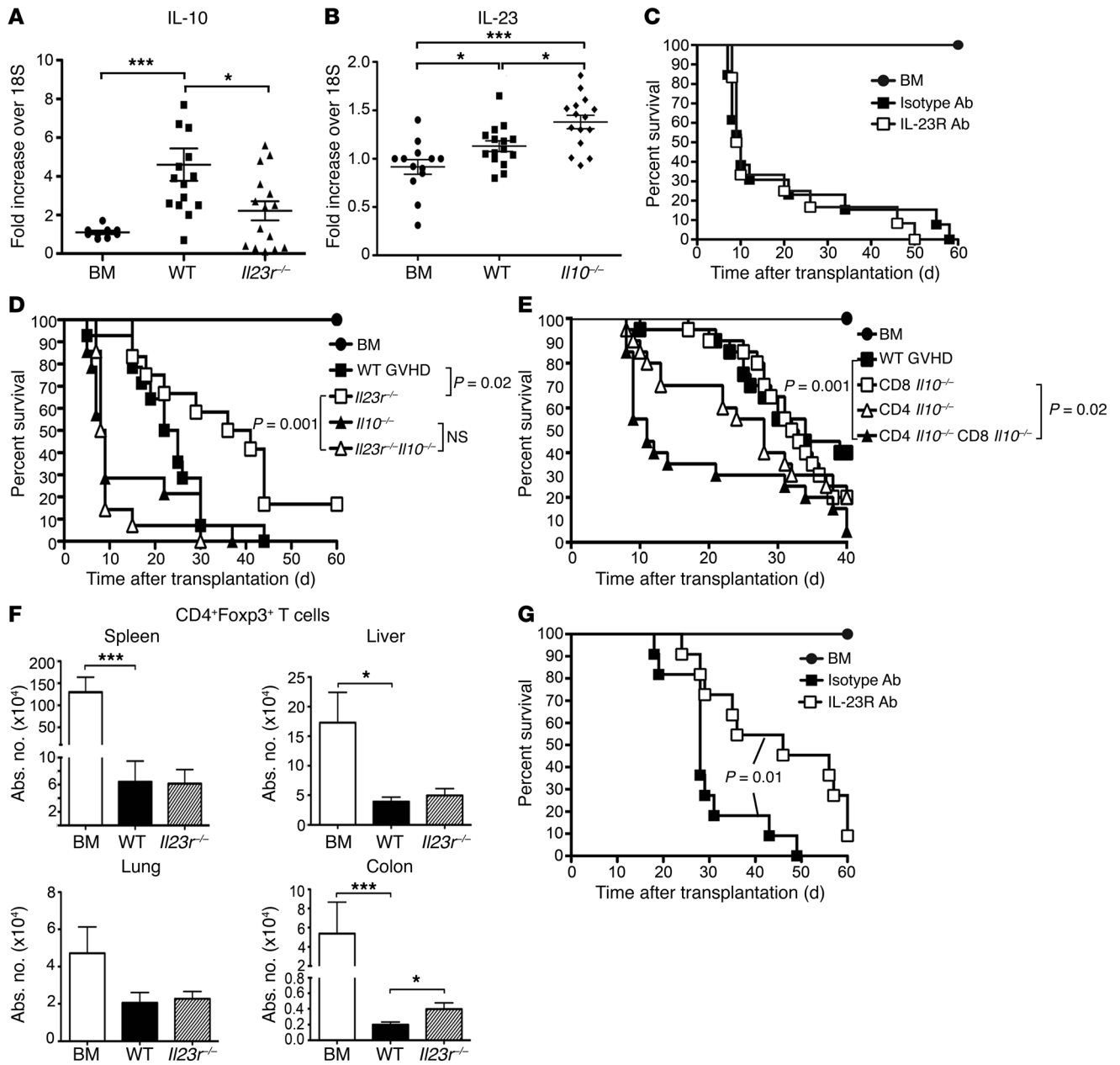


Figure 7. GVHD mediated by CD4⁺IL-23R⁺ T cells is regulated by IL-10 independently of CD4⁺Foxp3⁺ T cells. (A) IL-10 mRNA expression at 3 weeks in colons of BALB/c mice transplanted with Rag-1 BM (circles, $n = 9$) or BM and CD4⁺ T cells from B6 (squares, $n = 14$) or *Il23r^{-/-}* (triangles, $n = 15$) mice. (B) BALB/c animals transplanted with B6 BM (circles, $n = 13$), B6 BM and spleen cells (squares, $n = 15$), or *Il10^{-/-}* BM and *Il10^{-/-}* spleen cells (diamonds, $n = 15$). IL-23 mRNA expression in the colon. (C) BALB/c mice transplanted with *Il10^{-/-}* BM (black circles, $n = 9$) or transplanted with *Il10^{-/-}* spleen cells and treated with an isotype (black squares, $n = 14$) or anti-IL-23R (white squares, $n = 14$) antibody. (D) BALB/c mice transplanted with Rag-1 BM (black circles, $n = 9$) or BM and CD4⁺ T cells from B6 (black squares, $n = 14$), *Il23r^{-/-}* (white squares, $n = 14$), *Il10^{-/-}* (black triangles, $n = 14$), or *Il10^{-/-}* *Il23r^{-/-}* (white triangles, $n = 14$) T cells. (E) BALB/c mice transplanted with Rag-1 BM (black circles, $n = 12$), or with CD4⁺IL-10⁺ and CD8⁺IL-10⁺ (black squares, $n = 20$), CD4⁺IL-10⁺ and CD8⁺IL-10⁺ (white squares, $n = 20$), CD4⁺IL-10⁺ and CD8⁺IL-10⁻ (white triangles, $n = 20$), or CD4⁺IL-10⁻ and CD8⁺IL-10⁻ (black triangles, $n = 20$) T cells. (F) BALB/c animals transplanted with B6 BM (white bars) ($n = 6$) or BM and spleen cells from B6 (black bars) ($n = 10$) or *Il23r^{-/-}* (hatched bars) ($n = 12$) mice. The absolute number of CD4⁺Foxp3⁺ T cells at 4 weeks. (G) BALB/c mice transplanted with Rag-1 BM (black circles, $n = 4$) or with CD4⁺EGFP⁺ T cells (CD4 Δ) from Foxp3^{ΔEGFP} animals. Mice transplanted with CD4 Δ T cells treated with isotype (black squares, $n = 11$) or anti-IL-23R antibody (white squares, $n = 11$) weekly for 5 weeks. Data are from 3–4 experiments for each panel except G (2 experiments). Significant differences were calculated using the log rank test and 2-tailed Mann-Whitney *U* test. * $P < 0.05$, *** $P < 0.001$.

and that these animals had significantly prolonged survival relative to GVHD control mice reconstituted with whole CD4⁺ T cells (Figure 4E). To provide direct evidence that this CD4⁺ T cell phenotype could mediate lethal GVHD, mice were transplanted with BM cells

that were supplemented with CD4⁺ T cells that expressed CD11b and/or CD11c, or CD4⁺ T cells that lacked expression of these cell surface molecules. Overall survival was significantly worse in animals that were reconstituted with CD4⁺ T cells that expressed at

least 1 of these 2 integrins (Figure 4F). Finally, to determine whether the pathogenicity of β_2 integrin-expressing CD4⁺ T cells was dependent on the IL-23R, which was expressed at a higher level on these cells (Figure 3, D and F), experiments were performed in which animals were transplanted with CD4⁺ T cells that expressed CD11b and/or CD11c from wild-type or *Il23r*^{-/-} mice. Mice reconstituted with CD4⁺ *Il23r*^{-/-} T cells that expressed at least 1 β_2 integrin had significantly greater survival than animals transplanted with CD4⁺ *Il23r*^{+/+} T cells that had the same integrin profile (Figure 4G). Thus, these data indicated that the pathogenicity of β_2 integrin-expressing CD4⁺ T cells was dependent on coexpression of the IL-23R.

CD11c expression on CD4⁺IL-23R⁺ T cells defines a colitogenic phenotype. To define which β_2 integrin was most critical for inducing inflammation and lethality, CD4⁺ T cells were purified from *Cd11c*^{-/-} or *Cd11b*^{-/-} mice and transplanted into recipient animals. Notably, phenotypic examination prior to transplantation revealed that there was no difference in baseline IL-23R expression on naive CD4⁺ T cells from *Cd11b*^{-/-} or *Cd11c*^{-/-} mice (Figure 5A). Reconstitution with purified CD4⁺ T cells from *Cd11c*^{-/-} animals resulted in improved survival (Figure 5B) and significantly less weight loss (Figure 5C) relative to animals transplanted with wild-type CD4⁺ or CD4⁺ *Cd11b*^{-/-} T cells, indicating that CD11c expression on CD4⁺ T cells was important for in vivo pathogenicity. Animals reconstituted with CD4⁺ *Cd11c*^{-/-} T cells also had reduced pathological damage in all tissue sites, although differences were most significant in the colon (Supplemental Figure 4, A and B). Moreover, there was a significant decrease in the absolute number of total donor-derived CD4⁺, CD4⁺IL-23R⁺, CD4⁺IFN- γ ⁺, CD4⁺T-bet⁺, and CD4⁺TNF- α ⁺ T cells in the colon of these mice relative to the other cohorts (Supplemental Figure 4, C-F, and Supplemental Figure 5, A-D). Similar results were observed in an MHC-matched, minor antigen-mismatched GVHD model, indicating that these results were not strain specific (Supplemental Figure 6, A-C). We observed that CD4⁺ T cells from *Cd11c*^{-/-} mice did not differ from wild-type CD4⁺ T cells with respect to in vitro proliferation (Supplemental Figure 7A) or the ability to be polarized into Th1 or Th2 cytokine phenotypes (Supplemental Figure 7B). Thus, the transgenic environment did not alter these specific T cell parameters relative to CD4⁺ T cells from wild-type animals. Phenotypic analysis of CD4⁺CD11b⁺ and CD4⁺CD11c⁺ T cells from *Cd11c*^{-/-} and *Cd11b*^{-/-} mice, respectively (Supplemental Figure 8), revealed that only the latter had a biased central memory phenotype (Figure 5, D and E), similar to that observed in β_2 integrin-expressing cells from wild-type animals (Figure 3, B and C). Moreover, the IL-23R was expressed only on CD4⁺CD11c⁺ T cells with an effector or central memory phenotype and not on T cells with a naive phenotype (Supplemental Figure 9A). CD4⁺CD11c⁺ T cells also had increased expression of CCR9 and $\alpha_4\beta_7$ relative to CD4⁺CD11b⁺ T cells and to CD4⁺ T cells that lacked expression of either integrin (Figure 5F). Notably, CD4⁺CD11c⁺ T cells that expressed CCR9 or $\alpha_4\beta_7$ had a predominantly effector or central memory phenotype (Supplemental Figure 9B). A majority of CD4⁺CD11c⁺ T cells also expressed CCR7⁺, with most CCR7-expressing cells having a central memory T cell phenotype as well (Supplemental Figure 9B). Pathogenic CD4⁺IL-23R⁺ T cells were observed to downregulate CD62L after trafficking to the colon and had a largely effector memory phenotype (Supplemental Figure 9C).

To further characterize the CD4⁺CD11c⁺ T cell population from a functional perspective, we observed that there was an increased percentage of CD4⁺CD11c⁺ as opposed to CD4⁺CD11c⁻ T cells that produced IFN- γ when stimulated in the presence of IL-23 (Supplemental Figure 10A). IL-23 did not induce IL-17 in either cell population. Additionally, these cells were capable of responding to alloantigens in a fashion similar to that of CD4⁺CD11c⁻IL-23R⁻ central memory T cells, although proliferation was not as robust as observed for naive T cells (Supplemental Figure 10B). We then performed RNA sequencing (RNA-Seq) analysis on sorted CD4⁺CD11c⁺ (lacking coexpression of CD11b) and CD4⁺CD11c⁻ T cells obtained from wild-type mice to define the respective transcriptional profiles. These studies revealed a total of 587 differentially expressed genes of which 57 were downregulated and 530 were upregulated (Supplemental Figure 11A and Supplemental Table 1). This represented only 2.4% of 21,704 genes examined, which is in accord with prior reports of limited dissimilarity between naive and memory T cells (17). Using gene set enrichment analysis on the genes that had increased expression in the CD4⁺CD11c⁺ group yielded 4 notable annotation clusters by Database for Annotation, Visualization and Integrated Discovery (DAVID) analysis (Supplemental Table 2). Moreover, we observed that a number of genes that are commonly found in memory T cells were overexpressed in the CD4⁺CD11c⁺ T cell population (i.e., *H2Ab1*, *Dusp4*, *Cd74*, *Tnfrsf1b*, *S100a4*, *Tbet*, *Klrg1*, *Lgals3*, *Ifngr1*, and *CDKn1a*) (17) (Supplemental Figure 11B). A limitation of this approach, however, was that it compared a population with a diverse array of memory T cells with a CD11c⁺ population that was specifically enriched for central memory (CM) T cells. Therefore, we performed a more refined analysis to compare the respective transcriptional profiles of CD4⁺ CM T cells based on expression or absence of CD11c. This analysis of CD4⁺ CM T cells alone revealed a total of 684 differentially expressed genes of which 208 were downregulated and 476 were upregulated (Figure 5G and Supplemental Table 3). Gene set enrichment analysis of overexpressed genes yielded annotation clusters associated with antigen processing and immune response, whereas there was only 1 cluster that emerged in underexpressed genes (i.e., nucleosome) (Supplemental Table 4). CD4⁺CD11c⁺ CM T cells had increased expression of a number of class II genes (*H2Aa*, *H2Eb1*, *H2Eb2*, *H2DMA*, and *Cd74*) compared with CD4⁺CD11c⁻ CM T cells (Figure 5H). Additionally, these T cells had increased expression of the gut-homing molecule CCR9, which provided an explanation for their preferential ability to mediate inflammation in the GI tract. CD4⁺CD11c⁺ CM T cells also had expression of genes associated with the innate immune response (i.e., *Thr7*, *Thr12*, *Nod2*, and *Cd180*), as well as genes associated with dendritic cell populations (i.e., *Cd40*, *Clec9a*, *Cxcl16*, *Siglec*), suggesting that these T cells also had innate-like qualities. Collectively, these data indicated that CD11c expression defined a unique transcriptional profile within the CD4⁺ CM T cell population.

Donor-derived IL-10 regulates IL-23R-mediated GVHD and is produced primarily by non-Foxp3-expressing T cells. Since IL-10 has been shown to have a critical role in the maintenance of immune homeostasis within the colon (18, 19) and, similarly to IL-23, also signals through STAT3 (20), we hypothesized that IL-10 might regulate CD4⁺ IL-23R-mediated inflammation. Early after

transplantation, we observed that IL-10 levels were significantly increased in the serum of recipients of allogeneic as compared with syngeneic marrow grafts (Figure 6A), and that this disparity was relatively sustained during the first 3 weeks in comparison with IL-17 and IFN- γ . Donor (Figure 6B) but not host-derived IL-10 production (Figure 6C) was critical for mitigating GVHD lethality, as recipients of *Il10*^{-/-} grafts rapidly succumbed to death. Given the requirement for donor-derived IL-10, we used 10BiT.Foxp3^{EGFP} reporter mice to determine which donor cell populations produced this cytokine. Under steady-state conditions, T cells from normal 10BiT.Foxp3^{EGFP} reporter mice produced little IL-10 except in the colon, where approximately 70% of CD4⁺Foxp3⁺ and 15% of CD4⁺Foxp3⁻ T cells were IL-10⁺ (Supplemental Figure 12, A and B). Notably, fewer than 5% of conventional CD8⁺ T cells produced IL-10 in this tissue. To assess the effect of GVHD on IL-10 production, cohorts of animals were transplanted with syngeneic or allogeneic marrow grafts from IL-10 reporter mice. There were a significantly higher percentage and absolute number of IL-10⁺ cells observed in allogeneic recipients compared with syngeneic controls (Figure 6, D and E, and Supplemental Figure 13, A and B). Notably, the preponderance of IL-10 in GVHD target tissues derived almost exclusively from donor T cells (Figure 6D). In fact, only in the spleen was a significant non-T cell population identified that was IL-10⁺. IL-10 produced by CD4⁺ and CD8⁺ T cells in GVHD tissues was also detectable by immunoassay, providing confirmation that T cells were producing actual protein (Supplemental Figure 14). CD4⁺ and CD8⁺ Foxp3⁺ Tregs each constituted approximately 2%–3% of total CD4⁺ and CD8⁺ T cells early after transplantation in each organ (Figure 6E), and approximately 50% of these cells expressed IL-10 in mice undergoing GVHD. The absolute number of CD8⁺IL-10⁺ and CD4⁺IL-10⁺ Foxp3⁺ T cells was similar in all tissues, except the liver, where there were significantly more CD8⁺IL-10⁺ Tregs (Figure 6F). Notably, there was a substantial percentage of conventional CD4⁺ and CD8⁺ T cells that produced IL-10 in all organs (Figure 6, E and G). While the relative percentage of these cells that were IL-10⁺ was less than that for Foxp3-expressing T cells, the absolute number of IL-10-expressing conventional CD4⁺ and CD8⁺ T cells was at least 10-fold greater (Figure 6G). In addition, CD8⁺IL-10⁺Foxp3⁻ T cells were present in significantly greater numbers than CD4⁺IL-10⁺Foxp3⁻ T cells in all GVHD target organs, including the colon, identifying these cells as the major IL-10⁺ population.

GVHD mediated by CD4⁺IL-23R⁺ T cells is regulated by IL-10 independently of functional CD4⁺Foxp3⁺ T cells. Studies to further examine the role of IL-10 revealed that mice undergoing GVHD had a significant increase in IL-10 gene expression within the colon when compared with BM control animals, whereas animals transplanted with CD4⁺ *Il23r*^{-/-} T cells had a reduction in IL-10 mRNA levels (Figure 7A). Conversely, in the absence of donor-derived IL-10, IL-23 levels were increased in comparison with mice transplanted with wild-type marrow grafts (Figure 7B), suggesting that IL-10 production occurred in response to IL-23R-mediated proinflammatory effects. To determine whether this premise was correct, we examined whether GVHD protection occurring as a consequence of IL-23R signaling blockade was dependent on donor-derived IL-10. These studies revealed no difference in overall survival between animals transplanted with *Il10*^{-/-} marrow grafts and treat-

ed with either an isotype or anti-IL-23R antibody (Figure 7C), indicating that the survival advantage conferred by blockade of IL-23R signaling (Figure 1A) was abrogated when donor-derived cells were unable to produce IL-10. These results were confirmed using a genetic approach that demonstrated that, while animals reconstituted with CD4⁺ T cells from *Il23r*^{-/-} mice had a significant increase in survival relative to GVHD control mice, this effect was completely lost when mice were transplanted with CD4⁺ T cells from *Il10*^{-/-} *Il23r*^{-/-} donors (Figure 7D). To determine which IL-10-producing T cell population was most important for regulating GVHD lethality, experiments were performed in which animals were reconstituted with CD4⁺ and/or CD8⁺ T cells from either wild-type or *Il10*^{-/-} mice. These studies demonstrated that the accelerated GVHD mortality observed in the complete absence of donor-derived IL-10 was significantly reduced when CD4⁺IL-10⁺ T cells were present in the marrow graft (Figure 7E). In fact, these mice had survival that was not different from that of animals reconstituted with CD4⁺ and CD8⁺ T cells that were both IL-10 competent. Conversely, the presence of CD8⁺IL-10⁺ T cells alone had no protective effect, even though CD8⁺ T cells were the predominant IL-10-producing population early after transplantation (Figure 6G). Transplantation with CD4⁺ or CD8⁺ T cells alone from either wild-type or *Il10*^{-/-} mice also confirmed that only CD4⁺ T cell-derived IL-10 regulated GVHD lethality (Supplemental Figure 15).

CD4⁺Foxp3⁺ T cells have been shown to regulate GVHD (13), and secretion of IL-10 is 1 mechanism by which these cells mitigate disease severity (21). Given that IL-10 production by CD4⁺ T cells was critical for reducing GVHD, we sought to determine whether this was solely attributable to CD4⁺Foxp3⁺ Tregs. We observed that there was no difference in the number of CD4⁺Foxp3⁺ T cells present in the spleen, liver, or lung of animals that were transplanted with marrow grafts from wild-type or *Il23r*^{-/-} donors (Figure 7F). We did, however, observe a 2-fold increase in CD4⁺Foxp3⁺ T cell numbers in the colons of mice transplanted with *Il23r*^{-/-} grafts. Given this increase in Treg numbers within the colon coupled with the fact that the survival advantage conferred by IL-23R signaling blockade was attributable primarily to protection from colonic damage, we examined the requirement for CD4⁺ Tregs. To address this question, purified CD4⁺ T cells from Foxp3^{ΔEGFP} mice, which have a nonfunctional Foxp3 gene, were transplanted along with B6 Rag-1 BM into lethally irradiated mice, and then treated with either an isotype control or anti-IL-23R antibody. Animals to which anti-IL-23R antibody was administered had significantly prolonged survival relative to control mice (Figure 7G), indicating that GVHD protection occurring as a consequence of IL-23R signaling blockade did not require functional donor-derived CD4⁺Foxp3⁺ Tregs, and that IL-10 production by non-Foxp3-expressing CD4⁺ T cells was critical for preventing lethality.

Discussion

In the current study, using an experimental model of GVHD to examine T cell-mediated inflammation, we have identified a novel subset of CD4⁺ T cells that constitutively express the β_2 integrin CD11c, and shown that these cells potently induce inflammation in the colon. Notably, we observed that these cells have a biased central memory phenotype and transcriptional profile, as well as increased expression of the gut-homing molecules CCR9 and $\alpha_4\beta_7$,

which facilitated their ability to traffic into the colon microenvironment. The pathogenicity of these cells was critically dependent on coexpression of the IL-23R, which is augmented by the production of inflammatory cytokines such as IL-6 and IL-21 (22) that are increased in this tissue site during GVHD (23, 24). We initially observed that IL-23R expression was increased on CD4⁺ T cells that expressed CD11b and/or CD11c, raising the possibility that CD11c served only as a marker for a CD4⁺ T cell subpopulation that expressed the IL-23R, and did not confer additional pathogenic properties. However, the fact that baseline IL-23R expression was no different on CD4⁺ T cells from *Cd11b*^{-/-} and *Cd11c*^{-/-} animals, yet the former induced significantly greater mortality and pathological damage in the colon, is evidence that CD11c expression alone is important for *in vivo* pathogenicity independently of IL-23R expression. Thus, our data support a model whereby the coordinate expression of CD11c and the IL-23R on CD4⁺ T cells is critical for mediating maximal inflammation within the colon (Supplemental Figure 16).

Transcriptional profiling using RNA-Seq demonstrated that CD4⁺CD11c⁺ T cells from wild-type animals had a profile characterized by increased expression of genes commonly reported to be overexpressed in memory T cells (17), providing support for the premise that this was a unique central memory-biased CD4⁺ T cell population. Notably, a more refined transcriptional analysis that examined CD4⁺CD11c⁺ versus CD4⁺CD11c⁻ CM T cells revealed that the former T cell population had increased expression of CCR9, which provided an explanation for why these cells are particularly colitogenic. Furthermore, CD4⁺CD11c⁺ CM T cells also preferentially expressed genes associated with the innate immune response and dendritic cell populations, suggesting that they have innate-like properties. This would be a potential explanation for how a small population of CD4⁺ T cells could mediate a potent pathogenic effect by recognizing pathogen- or damage-associated molecular patterns that could amplify the early donor T cell response that we observed within the colon. Whether these cells are anatomically restricted to the spleen and lymph nodes or recirculate from the GI tract into secondary lymphoid tissues is not entirely clear, although the propensity of memory T cells to circulate from peripheral to secondary lymphoid tissues is well established and seems most plausible (25). Thus, we would posit that these cells become primed against self- or bacterial antigens in the GI tract and then are able to traffic back to the colon to mediate pathological damage under inflammatory conditions in which there are breakdown of mucosal barriers, loss of self-tolerance, and re-exposure to gut-associated antigens.

The role of memory T cells in the biology of GVHD has been an area of active investigation. A preponderance of preclinical studies has indicated that effector memory T cells have a markedly reduced ability to mediate GVHD when compared with naive T cells (26–28). The role of central memory T cells in the pathophysiology of GVHD, however, has been more controversial, as some studies have reported that these cells are able to cause GVHD (29, 30), while others have not observed a pathogenic role for this cell population (31). Notably, these studies have examined either unseparated central memory T cells or central memory CD8⁺ T cells, but have not directly examined the corresponding CD4⁺ T cell population. The results of this study further support an over-

all role for central memory T cells in the induction of GVHD and implicate a role for these cells in causing pathological damage within the GI tract. Transplantation of stem cell grafts depleted of naive T cells has recently been conducted in humans and has allowed one to indirectly assess the ability of memory T cells to cause GVHD, since these cells are enriched in the depleted stem cell product (32). A notable finding from this study was that while a majority of patients developed acute GVHD of the GI tract, it tended to be milder and more responsive to steroids than that observed after transplantation with stem cell grafts that also contained naive T cells. Thus, while this clinical study did not specifically examine central memory CD4⁺ T cells, this observation is compatible with the interpretation that memory T cells may have a proclivity to cause inflammation within the intestinal tract in humans as well.

Expression of β_2 integrins has been reported on effector CD8⁺ T cells, where this phenotype has been most commonly described in viral infections as a marker of recently activated or memory cells (33–35). However, the role of β_2 integrin-expressing CD4⁺ T cells has not been previously characterized. Known ligands for CD11c include ICAM-1, ICAM-2, collagen, and fibrinogen, which are all present in the microvasculature (36, 37) and are upregulated on both endothelial and epithelial cells in the GI tract during GVHD (38, 39). Therefore, adherence of CD4⁺CD11c⁺ T cells to these ligands could serve as a mechanism by which these cells enter into the colon and are then able to respond to other inflammatory cues that augment their pathogenicity. We observed that CD4⁺CD11c⁺ T cells from *Il23r*^{+/+} mice constituted a small proportion of total splenic and lymph node CD4⁺ T cells, and that only a small percentage CD4⁺IL-23R⁺ T cells were detectable in the colon, yet these cells were capable of inducing significant pathological damage and mortality. Another explanation for this finding emerged from the results of cotransfer experiments that revealed equivalent numbers of proinflammatory *Il23r*^{+/+} and *Il23r*^{-/-} T cells within the colon of GVHD mice, indicating that CD4⁺ *Il23r*^{-/-} T cells were capable of expansion and cytokine production in the colon, but were dependent on inflammatory signals delivered by CD4⁺IL-23R⁺ T cells. A similar premise has been advanced in an experimental model of inflammatory bowel disease (12). In previous studies (9), we demonstrated that IFN- γ was an important downstream mediator for IL-23-mediated pathological damage within the colon during GVHD. Therefore we surmise that increased IFN- γ production as a consequence of the augmented number of CD4⁺ *Il23r*^{-/-} T cells that accumulate in the presence of CD4⁺IL-23R⁺ T cells is a primary mechanism by which colonic inflammation is promoted.

IL-23 uses STAT3 as a cytoplasmic transcription factor that mediates downstream inflammatory events (40), but how this cytokine is regulated within the context of colonic inflammation is not well defined. Prior studies in murine models of inflammatory bowel disease and human colonic biopsies have demonstrated that an intact IL-23R signaling pathway is associated with decreased production of IL-10 (12, 41), implying that IL-23R signaling suppresses antiinflammatory pathways. In contrast to these studies, we observed that IL-10 levels in the serum and mRNA levels in the colon were significantly increased in mice with GVHD. Moreover, mice transplanted with CD4⁺ *Il23r*^{-/-} T cells had reduced IL-10 levels within the colon, supporting the premise that IL-10 production

serves as a counterregulatory response to IL-23R-mediated inflammation. The importance of IL-10 as a critical regulatory cytokine of IL-23R signaling was corroborated by the fact that transplantation with *Il10*^{-/-} grafts augmented GVHD mortality, blockade of IL-23R signaling was ineffectual in the absence of donor-derived IL-10 production, and transplantation with CD4⁺ T cells from *Il23r*^{-/-} *Il10*^{-/-} animals abrogated the protection that was observed when animals were reconstituted with *Il23r*^{-/-} T cells alone. Thus, a critical role of IL-10 appears to be the suppression of inflammation mediated by CD4⁺CD11c⁺ T cells through the IL-23R signaling pathway. How IL-10 directly regulates IL-23 is not entirely clear, although a potential regulatory pathway may involve *Nfil3*, an IL-10-inducible gene (42) that has been shown to inhibit IL-12/23-mediated colitis in immunodeficient animals (43). Therefore, in the absence of IL-10 production by CD4⁺ T cells, NFIL3 transcription would be predicted to be decreased, which could lead to enhanced inflammation through the IL-23 signaling pathway.

IL-10 production by Tregs has been demonstrated, in a number of experimental models (44, 45), including GVHD (21, 46), to be important for the maintenance of tolerance and the amelioration of inflammatory responses. Moreover, IL-10 production by non-Foxp3-expressing CD4⁺ T cells, termed Tr1 cells, has also been shown to mitigate inflammation in models of autoimmunity and chronic inflammation (47). Although we observed that IL-10-expressing Tregs were indeed present in all target tissues, the majority of IL-10⁺ cells were non-Foxp3-expressing T cells, primarily CD8⁺ T cells. Furthermore, blockade of IL-23R signaling was able to prolong survival in the complete absence of CD4⁺ Tregs, indicating that, in contrast to IL-10, there was not a strict requirement for Tregs to observe a protective effect from IL-23R signaling inhibition. T cell subset transfer studies designed to determine the T cell population that was critical for the production of IL-10 and amelioration of GVHD severity revealed that non-Foxp3-expressing CD4⁺ T cells were actually most responsible for the mitigation of GVHD. Notably, CD4⁺ T cells obtained from GVHD target tissues also produced higher levels of IL-10 in vitro than the corresponding CD8⁺ T cell population, providing an explanation for why these cells might be more potent in vivo. Thus, while non-Foxp3-expressing CD8⁺IL-10⁺ T cells have been shown to exert a dominant suppressive role in other settings (48), they did not mediate any apparent protective effect, despite being present in significantly higher absolute numbers in all tissue sites. An explanation for these results is that the 10BiT.Foxp3^{EGFP} reporter mouse quantifies not the amount of IL-10 produced, but rather only the percentage of cells that have been programmed to make IL-10. Therefore, our data would support the interpretation that non-Foxp3-expressing CD4⁺ T cells produced more IL-10 on a per-cell basis. While these results do not exclude a role for Treg-derived IL-10 in GVHD prevention, by either donor or residual radioresistant recipient populations, they indicate that IL-10 production by non-Foxp3-expressing CD4⁺ T cells appeared to be critical for the regulation of colonic inflammation in this setting.

From a clinical perspective, blockade of the IL-23 signaling pathway is a potentially viable strategy to reduce the severity of GVHD in the GI tract, which remains a major cause of morbidity in allogeneic hematopoietic stem cell transplant recipients. Anecdotal reports (49) have demonstrated activity of ustekinumab,

which blocks the p40 subunit that is shared by IL-12 and IL-23 and has been shown to have a role in the pathophysiology of GVHD (50). However, given that IL-12 has other critical immunological functions (51), the more selective blockade of IL-23 through its p19 subunit or unique receptor may be a more rational strategy to prevent gastrointestinal GVHD and warrants further investigation. This would likely be a more effective strategy than one directed at attempting to deplete CD11c-expressing CD4⁺ T cells given that this molecule is also expressed on dendritic cell populations, which could lead to other potentially undesirable effects with respect to immune competency and antileukemia reactivity.

In summary, we have identified a novel population of CD4⁺ T cells that constitutively express the β_2 integrin CD11c and have a biased central memory phenotype and transcriptional profile, increased expression of gut-homing molecules, and the ability to potently drive inflammation within the colon. These cells also had a gene expression profile with both innate and adaptive characteristics, providing a potential explanation for why these cells play an important role in early colonic inflammation. The ability of these cells to mediate pathological damage was critically dependent on the coordinate expression of the IL-23R in the colon microenvironment, which served to further augment inflammation and facilitate the expansion of *Il23r*^{-/-} T cell populations. The role of these cells in driving early inflammatory events in colonic GVHD suggests that they may have a wider role in the pathogenesis of immune-mediated inflammatory bowel diseases in rodents and potentially humans.

Methods

Mice. C57BL/6 (B6) (H-2^b), BALB/c (H-2^d), B6.PL (H-2^b, Thy1.1⁺), B6.SJL (CD45.1⁺), B6 Foxp3^{EGFP}, B6 *Rag1*^{-/-}, BALB.B (H-2^b), *Cd11b*^{-/-}, B6 *Il10*^{-/-}, and BALB/c *Il10*^{-/-} mice were bred in the Animal Resource Center (ARC) at the Medical College of Wisconsin or purchased from The Jackson Laboratory. Foxp3^{ΔEGFP} mice, in which there is mutation in the Foxp3 coding region that renders the Foxp3 gene nonfunctional, have been reported (52). *Il23r*^{-/-}, *Cd11c*^{-/-}, and IL-10BiT-Foxp3^{EGFP} reporter mice have also been described (53–55). *Il23r*^{-/-} *Il10*^{-/-} animals were made by intercrossing of *Il23r*^{-/-} × *Il10*^{-/-} heterozygotes and screening for homozygosity by PCR. All animals were housed in the Association for Assessment and Accreditation of Laboratory Animal Care-accredited ARC of the Medical College of Wisconsin. Mice received regular mouse chow and acidified tap water ad libitum.

Reagents. Anti-IL-23R antibody is a mouse IgG antibody that has been previously described (56). Animals received a dose of 0.75 mg i.p. on the day of transplantation prior to irradiation and then were treated with 0.75 mg weekly by i.p. injection for 4 additional weeks. Mouse IgG (Merck Pharmaceuticals) was used as a control and administered at the same dose and schedule as anti-IL-23R antibody. Antibodies were resuspended in PBS before injection.

BM transplantation. Bone marrow (BM) was flushed from donor femurs and tibias with DMEM (Gibco-BRL) and passed through sterile mesh filters to obtain single-cell suspensions. Host mice were conditioned with total-body irradiation administered as a single exposure of 900–1,000 cGy at a dose rate of 74 cGy/min using a Shepherd Mark I Cesium Irradiator (J.L. Shepherd and Associates). Irradiated recipients received a single i.v. injection in the lateral tail vein of BM (10 × 10⁶) with or without added spleen or purified T cells. T cells were puri-

fied by magnetic beads using a pan-T cell isolation column (Miltenyi Biotec), or by cell sorting. Mice were weighed 2–3 times per week and were euthanized when they attained predefined morbidity criteria. In experiments that used Foxp3^{EGFP} mice as donors, CD45.2⁺CD4⁺EGFP⁺ T cells were sorted from the spleens of reconstituted animals before transplantation.

Isolation of lymphocyte populations. Lamina propria lymphocytes were isolated from colon samples using the Lamina Propria Dissociation Kit (Miltenyi Biotec) according to the manufacturer's instructions. The resulting cell suspension was then layered on a 44%/67% Percoll gradient (Sigma-Aldrich). Liver and lung lymphocytes were isolated by collagenase D digestion followed by layering on a Percoll gradient.

Cell sorting and flow cytometry. Spleen and peripheral lymph node cells from mice were sorted on a FACSAria (Becton Dickinson). Lymphocytes from spleen, liver, colon, and lung were labeled with mAbs conjugated to fluorescent dyes as listed in Supplemental Table 5. 7-Aminoactinomycin was used to exclude dead cells. Cells were analyzed on a BD LSRII flow cytometer with FACSDiva software (Becton Dickinson). Data were analyzed using FlowJo software (Tree Star).

T cell proliferation and polarization assays. For proliferation experiments, naive CD4⁺CD62L⁺CD44⁻ spleen cells were sorted and loaded with Cell Trace Violet dye (Invitrogen). Cells were then cultured for 3 days in complete DMEM supplemented with 10% FBS (Atlanta Biologicals), 1× penicillin/streptomycin/glutamine, 1× nonessential amino acids, 1× sodium pyruvate, 10 mM HEPES, 50 μM 2-mercaptoethanol (Invitrogen), 1 μg/ml anti-CD28 antibody (BD Pharmingen), and 20 U human IL-2 in a flat-bottom 96-well plate coated with 5 μg/ml anti-CD3 antibody (BD Pharmingen). For cell polarization studies, naive spleen cells were cultured in anti-CD3 antibody-coated flat-bottom 96-well plates in complete DMEM containing anti-CD28 antibody and IL-2 with either 20 ng/ml IL-12 and 10 ng/ml anti-IL-4 antibody (Biolegend) (Th1 conditions), or 100 ng/ml IL-4 (Shenandoah Biotechnology), 10 ng/ml anti-IFN-γ antibody (BD Biosciences), and 10 ng/ml anti-IL-12 antibody (Biolegend) (Th2 conditions). Cells were cultured for 48 hours, at which point they were transferred to a new plate and cultured for an additional 3 days. On day 5, cells were stained for intracellular IFN-γ and IL-4.

Mixed lymphocyte culture. Sorted CD4⁺ T cell populations (2.5 × 10⁴ to 3 × 10⁴) were labeled with Cell Trace Violet and then cocultured with 1.5 × 10⁴ BALB/c dendritic cell-enriched stimulator cells in V-bottomed microwell plates (Becton Dickinson) at 37°C for 4 days. Stimulator cells were obtained by digestion of spleens with collagenase D (1 mg/ml) followed by positive selection of CD11c⁺ cells using the magnetic activated cell sorting system.

Serum cytokine measurements. Serum was collected from mice by retro-orbital bleeds and analyzed using a Bio-Plex System (Bio-Rad Laboratories) according to the manufacturer's instructions.

Intracellular cytokine staining. Lymphocytes isolated from the colon were stimulated with 50 ng/ml phorbol 12-myristate 13-acetate (PMA; Sigma-Aldrich) and 750 ng/ml ionomycin (Calbiochem) for 1 hour and then incubated with GolgiStop (BD Pharmingen) for an additional 4 hours. In other experiments, splenic T cells were stimulated with PMA and ionomycin plus IL-23 (20 ng/ml) overnight and incubated with GolgiStop for a total of 18 hours. Cells were surface stained and then intracellularly stained with mAbs listed in Supplemental Table 5.

Immunoassay. IL-10 was measured using the quantitative Bio-Plex Mouse Cytokine IL-10 assay (Bio-Rad Laboratories) according

to the manufacturer's instructions. In brief, sorted CD4⁺ or CD8⁺ T cells were activated with PMA/ionomycin plus 30 U/ml of IL-2 overnight. Supernatants were harvested from activated T cell cultures, and murine IL-10 was detected using magnetically coupled anti-IL-10 beads, biotinylated detection antibodies, and a reporter streptavidin-phycoerythrin conjugate. Data were collected and analyzed using a Bio-Plex 200 instrument equipped with BioManager 6.0 analysis software (Bio-Rad Laboratories).

Human mixed lymphocyte cultures. Mixed lymphocyte cultures were performed using peripheral blood mononuclear cells (PBMCs) obtained from healthy blood donor buffy coat units after density gradient separation (Biocoll; Merck Millipore). Peripheral blood lymphocytes were prepared from PBMCs by incubation in T25 flasks at 37°C for 4 hours to overnight and removal of nonadherent cells. Peripheral blood lymphocyte responders were cultured in RPMI-1640 (25 mM HEPES/2 mM L-glutamine)/10% single-donor human AB serum (GemCell; Gemini Bio-Products) and were admixed at a 1:1 ratio with 30-Gy-irradiated PBMCs from a fully allogeneic donor. A total of 10 ml of the cell mixture was incubated at 37°C in T25 tissue culture flasks in a humidified atmosphere of 5% CO₂ for a period of 7–8 days. After incubation, cells were washed from culture, centrifuged over density gradient medium, and phenotyped for the expression of CD11b and CD11c on CD3⁺CD4⁺ T cells. Nonstimulated control cells were phenotyped before incubation.

Histological analysis. Representative samples of liver, colon, and lung were obtained from transplanted recipients and fixed in 10% neutral-buffered formalin. Samples were then embedded in paraffin, cut into 5-μm-thick sections, and stained with H&E. A semiquantitative scoring system was used to account for histological changes in the colon, liver, and lung as previously described (9, 23). All slides were coded and read in a blinded fashion. Images were visualized with an Olympus BX45 microscope. Image acquisition was performed with an Olympus DP70 digital camera and software package.

RNA isolation, cDNA synthesis, and real-time quantitative PCR. Total RNA was homogenized from flash-frozen tissues collected from transplant recipients using Trizol Reagent (Life Technologies) followed by isopropyl alcohol precipitation. cDNA was synthesized using the QuantiTect Reverse Transcription Kit (Qiagen) according to the manufacturer's protocol. Real-time quantitative RT-PCR was performed using QuantiFast SYBR Green PCR Kit (Qiagen) and run in a CFX C1000 Real-Time Thermal Cycler (Bio-Rad Laboratories). The 18S reference gene was amplified using the QuantiTect Primer Assay Kit (Qiagen). The primers for IL-23 (forward 5'-AGCGGGACATATGAATCTACTAAGAGA-3', reverse 5'-GTCCTAGTAGGGAGGTGTGAAGTTG-3') and IL-10 (forward 5'-ATGCTGCCTGCTCTTACTGACTG-3', reverse 5'-CCCAAGTAACCCTTAAAGTCCTGC-3') were purchased from Integrated DNA Technologies. Specificity for all quantitative RT-PCR reactions was verified by melting curve analysis. To calculate fold change in gene expression, the average ΔΔCt values from triplicate wells were combined from separate experiments.

RNA sequence analysis. RNA was extracted from flow-sorted CD4⁺CD11c⁻ (2.6 × 10⁶ to 3.2 × 10⁶) or CD4⁺CD11c⁺ (2.75 × 10⁴ to 4.25 × 10⁴) T cells using the RNeasy Mini Kit (Qiagen), and mRNA sequencing libraries were prepared according to the TruSeq protocol (Illumina). For mRNA sequencing, samples were processed as previously described by the Cancer Genome Atlas (57) and sequenced on 1 lane of an Illumina HiSeq2500 with 2 × 50 paired-end sequencing chemistry.

Bases and quality control assessment of sequencing were generated by CASAVA 1.8 (Illumina). Quality control-passed reads were aligned to the mouse reference genome using MapSplice (58). Aligned reads were sorted and indexed using SAMtools (<http://www.htslib.org>), and then translated to transcriptome coordinates and filtered for large inserts and zero mapping quality using UBU 1.0 (<https://github.com/mozack/ubu>). For the reference transcriptome, University of California, Santa Cruz, mouse Known Genes (59) was used, with genes located on nonstandard chromosomes removed. The abundance of transcripts was then estimated using an Expectation-Maximization algorithm implemented in the software package RSEM 1.1.13 (60). Estimated counts were normalized to the upper quartile (61) before comparison of expression across protocols. Genes were tested for significant differences in expression between groups using Welch's *t* tests with Bonferroni correction for multiple testing, implemented in the multtest R package (Team RDC, 2011; ref. 62). Significantly differentially expressed genes were taken to be those for which the Bonferroni-adjusted *P* value was less than 0.05, and expression values of these genes were displayed as a heatmap made using the heatmap.2 function in the gplots R package, with cluster method "complete" and distance method "Euclidean" (Team RDC, 2011; ref. 63).

Gene set enrichment analysis. Differentially expressed genes were tested for gene set and pathway enrichment using the DAVID software tool (64, 65). GOTERM_BP_FAT (gene ontology), KEGG (pathways), and INTERPRO (protein domains) were used as search terms. Significance was defined as *P* value adjusted by FDR of less than or equal to 0.05.

Accession numbers. Accession numbers are as follows: CD11c⁺ P1 (GSM2209500); CD11c⁺ P2 (GSM2209501); CD11c⁺ P3 (GSM2209502); CD11c⁻ P1 (GSM2209503); CD11c⁻ P2 (GSM2209504); CD11c⁻ P3 (GSM2209505).

Statistics. Group comparisons of T cell populations, cytokine levels, pathology scores, and gene expression data were performed using the nonparametric 2-tailed Mann-Whitney *U* test. Survival curves were constructed using the Kaplan-Meier product limit estimator and compared using the log rank test. A *P* value of ≤0.05 was considered significant.

Study approval. All experiments were reviewed and approved by the Institutional Animal Care and Use Committee of the Medical College of Wisconsin (Milwaukee, Wisconsin, USA).

Author contributions

VZ is a co-first author who performed animal studies and flow cytometric analysis and helped write the manuscript. KA is a co-first author who performed animal studies, conducted flow cytometry, generated figures, and helped write the manuscript. XC, LB, and AB performed animal studies. CT and FZ performed human mixed lymphocyte culture studies. DAS, BV, and JS performed RNA sequence analysis. WB, SS, EB, DH, CBW, JV, CW, CB, and DJC provided critical reagents and edited the paper. RK performed pathological analysis of all tissue samples. WRD developed the overall concept, designed experiments, supervised the study, and wrote the manuscript.

Acknowledgments

This research was supported by grants from the NIH (HL126166 and HL064603) and by awards from the Midwest Athletes Against Childhood Cancer Fund.

Address correspondence to: William R. Drobyski, Bone Marrow Transplant Program, 8701 Watertown Plank Road, Milwaukee, Wisconsin 53226, USA. Phone: 414.456.4941; E-mail: wdrobysk@mcw.edu.

- Shlomchik WD. Graft-versus-host disease. *Nat Rev Immunol.* 2007;7(5):340–352.
- Welniak LA, Blazar BR, Murphy WJ. Immunobiology of allogeneic hematopoietic stem cell transplantation. *Annu Rev Immunol.* 2007;25:139–170.
- Ferrara JL, Levine JE, Reddy P, Holler E. Graft-versus-host disease. *Lancet.* 2009;373(9674):1550–1561.
- Hill GR, Crawford JM, Cooke KR, Brinson YS, Pan L, Ferrara JL. Total body irradiation and acute graft-versus-host disease: the role of gastrointestinal damage and inflammatory cytokines. *Blood.* 1997;90(8):3204–3213.
- Teshima T, et al. Acute graft-versus-host disease does not require alloantigen expression on host epithelium. *Nat Med.* 2002;8(6):575–581.
- Carlson MJ, West ML, Coghill JM, Panoskaltis-Mortari A, Blazar BR, Serody JS. In vitro-differentiated TH17 cells mediate lethal acute graft-versus-host disease with severe cutaneous and pulmonary pathologic manifestations. *Blood.* 2009;113(6):1365–1374.
- Hill GR, Ferrara JL. The primacy of the gastrointestinal tract as a target organ of acute graft-versus-host disease: rationale for the use of cytokine shields in allogeneic bone marrow transplantation. *Blood.* 2000;95(9):2754–2759.
- Cooke KR, et al. LPS antagonism reduces graft-versus-host disease and preserves graft-versus-leukemia activity after experimental bone marrow transplantation. *J Clin Invest.* 2001;107(12):1581–1589.
- Das R, Chen X, Komorowski R, Hessner MJ, Drobyski WR. Interleukin-23 secretion by donor antigen-presenting cells is critical for organ-specific pathology in graft-versus-host disease. *Blood.* 2009;113(10):2352–2362.
- Uhlir HH, et al. Differential activity of IL-12 and IL-23 in mucosal and systemic innate immune pathology. *Immunity.* 2006;25(2):309–318.
- Parham C, et al. A receptor for the heterodimeric cytokine IL-23 is composed of IL-12Rβ1 and a novel cytokine receptor subunit, IL-23R. *J Immunol.* 2002;168(11):5699–5708.
- Ahern PP, et al. Interleukin-23 drives intestinal inflammation through direct activity on T cells. *Immunity.* 2010;33(2):279–288.
- Taylor PA, Lees CJ, Blazar BR. The infusion of ex vivo activated and expanded CD4(+)CD25(+) immune regulatory cells inhibits graft-versus-host disease lethality. *Blood.* 2002;99(10):3493–3499.
- Schneidawind D, Pierini A, Negrin RS. Regulatory T cells and natural killer T cells for modulation of GVHD following allogeneic hematopoietic cell transplantation. *Blood.* 2013;122(18):3116–3121.
- Beres AJ, Haribhai D, Chadwick AC, Gonyo PJ, Williams CB, Drobyski WR. CD8⁺ Foxp3⁺ regulatory T cells are induced during graft-versus-host disease and mitigate disease severity. *J Immunol.* 2012;189(1):464–474.
- Robb RJ, et al. Identification and expansion of highly suppressive CD8(+)FoxP3(+) regulatory T cells after experimental allogeneic bone marrow transplantation. *Blood.* 2012;119(24):5898–5908.
- Weng NP, Araki Y, Subedi K. The molecular basis of the memory T cell response: differential gene expression and its epigenetic regulation. *Nat Rev Immunol.* 2012;12(4):306–315.
- Kühn R, Löhler J, Rennick D, Rajewsky K, Müller W. Interleukin-10-deficient mice develop chronic enterocolitis. *Cell.* 1993;75(2):263–274.
- Davidson NJ, et al. T helper cell 1-type CD4⁺ T cells, but not B cells, mediate colitis in interleukin 10-deficient mice. *J Exp Med.* 1996;184(1):241–251.
- Saraiva M, O'Garra A. The regulation of IL-10 production by immune cells. *Nat Rev Immunol.* 2010;10(3):170–181.
- Hoffmann P, Ermann J, Edinger M, Fathman CG, Strober S. Donor-type CD4(+)CD25(+) regulatory T cells suppress lethal acute graft-versus-host disease after allogeneic bone marrow transplantation. *J Exp Med.* 2002;196(3):389–399.
- Zhou L, et al. IL-6 programs T(H)-17 cell differentiation by promoting sequential engagement of the IL-21 and IL-23 pathways. *Nat Immunol.* 2007;8(9):967–974.
- Chen X, et al. Blockade of interleukin-6 signaling

- augments regulatory T-cell reconstitution and attenuates the severity of graft-versus-host disease. *Blood*. 2009;114(4):891–900.
24. Bucher C, et al. IL-21 blockade reduces graft-versus-host disease mortality by supporting inducible T regulatory cell generation. *Blood*. 2009;114(26):5375–5384.
 25. Mueller SN, Gebhardt T, Carbone FR, Heath WR. Memory T cell subsets, migration patterns, and tissue residence. *Annu Rev Immunol*. 2013;31:137–161.
 26. Anderson BE, et al. Memory CD4⁺ T cells do not induce graft-versus-host disease. *J Clin Invest*. 2003;112(1):101–108.
 27. Zheng H, et al. Effector memory CD4⁺ T cells mediate graft-versus-leukemia without inducing graft-versus-host disease. *Blood*. 2008;111(4):2476–2484.
 28. Zhang P, Wu J, Deoliveira D, Chao NJ, Chen BJ. Allo-specific CD4(+) effector memory T cells do not induce graft-versus-host disease in mice. *Biol Blood Marrow Transplant*. 2012;18(10):1488–1499.
 29. Zhang Y, Joe G, Hexner E, Zhu J, Emerson SG. Alloreactive memory T cells are responsible for the persistence of graft-versus-host disease. *J Immunol*. 2005;174(5):3051–3058.
 30. Zheng H, Matte-Martone C, Jain D, McNiff J, Shlomchik WD. Central memory CD8⁺ T cells induce graft-versus-host disease and mediate graft-versus-leukemia. *J Immunol*. 2009;182(10):5938–5948.
 31. Chen BJ, et al. Inability of memory T cells to induce graft-versus-host disease is a result of an abortive alloresponse. *Blood*. 2007;109(7):3115–3123.
 32. Bleakley M, et al. Outcomes of acute leukemia patients transplanted with naive T cell-depleted stem cell grafts. *J Clin Invest*. 2015;125(7):2677–2689.
 33. Christensen JE, Andreasen SO, Christensen JP, Thomsen AR. CD11b expression as a marker to distinguish between recently activated effector CD8(+) T cells and memory cells. *Int Immunol*. 2001;13(4):593–600.
 34. McFarland HI, Nahill SR, Maciaszek JW, Welsh RM. CD11b (Mac-1): a marker for CD8⁺ cytotoxic T cell activation and memory in virus infection. *J Immunol*. 1992;149(4):1326–1333.
 35. Sadhu C, et al. CD11c/CD18: novel ligands and a role in delayed-type hypersensitivity. *J Leukoc Biol*. 2007;81(6):1395–1403.
 36. Frick C, et al. Interaction of ICAM-1 with β 2-integrin CD11c/CD18: characterization of a peptide ligand that mimics a putative binding site on domain D4 of ICAM-1. *Eur J Immunol*. 2005;35(12):3610–3621.
 37. Lin Y, Roberts TJ, Sriram V, Cho S, Brutkiewicz RR. Myeloid marker expression on antiviral CD8⁺ T cells following an acute virus infection. *Eur J Immunol*. 2003;33(10):2736–2743.
 38. Blazar BR, Taylor PA, Panoskaltis-Mortari A, Gray GS, Vallera DA. Coblockade of the LFA1: ICAM and CD28/CTLA4:B7 pathways is a highly effective means of preventing acute lethal graft-versus-host disease induced by fully major histocompatibility complex-disparate donor grafts. *Blood*. 1995;85(9):2607–2618.
 39. Eyrich M, et al. Sequential expression of adhesion and costimulatory molecules in graft-versus-host disease target organs after murine bone marrow transplantation across minor histocompatibility antigen barriers. *Biol Blood Marrow Transplant*. 2005;11(5):371–382.
 40. Yang XO, et al. STAT3 regulates cytokine-mediated generation of inflammatory helper T cells. *J Biol Chem*. 2007;282(13):9358–9363.
 41. Liu Z, Feng BS, Yang SB, Chen X, Su J, Yang PC. Interleukin (IL)-23 suppresses IL-10 in inflammatory bowel disease. *J Biol Chem*. 2012;287(5):3591–3597.
 42. Lang R, Patel D, Morris JJ, Rutschman RL, Murray PJ. Shaping gene expression in activated and resting primary macrophages by IL-10. *J Immunol*. 2002;169(5):2253–2263.
 43. Kobayashi T, et al. NFIL3-deficient mice develop microbiota-dependent, IL-12/23-driven spontaneous colitis. *J Immunol*. 2014;192(4):1918–1927.
 44. Rubtsov YP, et al. Regulatory T cell-derived interleukin-10 limits inflammation at environmental interfaces. *Immunity*. 2008;28(4):546–558.
 45. Chaudhry A, et al. Interleukin-10 signaling in regulatory T cells is required for suppression of Th17 cell-mediated inflammation. *Immunity*. 2011;34(4):566–578.
 46. Tawara I, et al. Donor- but not host-derived interleukin-10 contributes to the regulation of experimental graft-versus-host disease. *J Leukoc Biol*. 2012;91(4):667–675.
 47. Huber S, et al. Th17 cells express interleukin-10 receptor and are controlled by Foxp3⁺ and Foxp3⁻ regulatory CD4⁺ T cells in an interleukin-10-dependent manner. *Immunity*. 2011;34(4):554–565.
 48. Sun J, Madan R, Karp CL, Braciale TJ. Effector T cells control lung inflammation during acute influenza virus infection by producing IL-10. *Nat Med*. 2009;15(3):277–284.
 49. Pidala J, Perez L, Beato F, Anasetti C. Ustekinumab demonstrates activity in glucocorticoid-refractory acute GVHD. *Bone Marrow Transplant*. 2012;47(5):747–748.
 50. Wu Y, et al. Essential role of interleukin-12/23p40 in the development of graft-versus-host disease in mice. *Biol Blood Marrow Transplant*. 2015;21(7):1195–1204.
 51. Vignali DA, Kuchroo VK. IL-12 family cytokines: immunological playmakers. *Nat Immunol*. 2012;13(8):722–728.
 52. Lin W, et al. Regulatory T cell development in the absence of functional Foxp3. *Nat Immunol*. 2007;8(4):359–368.
 53. Chan JR, et al. IL-23 stimulates epidermal hyperplasia via TNF and IL-20R2-dependent mechanisms with implications for psoriasis pathogenesis. *J Exp Med*. 2006;203(12):2577–2587.
 54. Wu H, et al. Deficiency of CD11b or CD11d results in reduced staphylococcal enterotoxin-induced T cell response and T cell phenotypic changes. *J Immunol*. 2004;173(1):297–306.
 55. Maynard CL, et al. Regulatory T cells expressing interleukin 10 develop from Foxp3⁺ and Foxp3⁻ precursor cells in the absence of interleukin 10. *Nat Immunol*. 2007;8(9):931–941.
 56. McGeachy MJ, et al. The interleukin 23 receptor is essential for the terminal differentiation of interleukin 17-producing effector T helper cells in vivo. *Nat Immunol*. 2009;10(3):314–324.
 57. Cancer Genome Atlas Research Network, et al. The Cancer Genome Atlas Pan-Cancer analysis project. *Nat Genet*. 2013;45(10):1113–1120.
 58. Wang K, et al. MapSplice: accurate mapping of RNA-seq reads for splice junction discovery. *Nucleic Acids Res*. 2010;38(18):e178.
 59. Karolchik D, et al. The UCSC Genome Browser database: 2014 update. *Nucleic Acids Res*. 2014;42(Database issue):D764–D770.
 60. Li B, Dewey CN. RSEM: accurate transcript quantification from RNA-Seq data with or without a reference genome. *BMC Bioinformatics*. 2011;12:323.
 61. Bullard JH, Purdom E, Hansen KD, Dudoit S. Evaluation of statistical methods for normalization and differential expression in mRNA-Seq experiments. *BMC Bioinformatics*. 2010;11:94.
 62. Pollard KS, Dudoit S, van der Laan MJ. Multiple testing procedures: R multtest package and applications to genomics. In: Gentleman R, Carey V, Huber W, Irizarry R, Dudoit S, eds. *Bioinformatics and Computational Biology Solutions Using R and Bioconductor*. New York, New York, USA: Springer (Statistics for Biology and Health Series); 2005:251–272.
 63. Warnes GR, et al. gplots: various R Programming Tools for Plotting Data. R package version 2.17.0. CRAN-Package gplot Web site. <http://CRAN.R-project.org/package=gplots>. Updated March 30, 2016. Accessed July 7, 2016.
 64. Huang da W, Sherman BT, Lempicki RA. Bioinformatics enrichment tools: paths toward the comprehensive functional analysis of large gene lists. *Nucleic Acids Res*. 2009;37(1):1–13.
 65. Huang DW, Sherman BT, Lempicki RA. Systematic and integrative analysis of large gene lists using DAVID bioinformatics resources. *Nat Protoc*. 2009;4(1):44–57.